Aus der Klinik für Kardiologie
des Deutschen Herzzentrum Berlin
DISSERTATION

Metabolic profiling in experimental autoimmune myocarditis (EAM) in a rodent model using ex-vivo proton magic angle spinning magnetic resonance spectroscopy (1H-MAS-MRS) to detect myocardial injury.

zur Erlangung des akademischen Grades
Doctor medicinae (Dr. med.)

vorgelegt der Medizinischen Fakultät
Charité – Universitätsmedizin Berlin

von

Frédéric Münch,
aus Bad Säckingen.

Datum der Promotion: 22.09.2017

Table of Contents

Abstract

Background. Myocarditis is an inflammatory disease of the myocardium that can lead to dilated cardiomyopathy (DCM) and heart failure (HF). Experimental autoimmune myocarditis (EAM) in rodents is an accepted model of myocarditis and DCM. Altered cellular metabolism is thought to play an important role in the pathogenesis of DCM and generally in HF. Study of the metabolism may provide new diagnostic information and insights into the mechanisms of myocarditis and HF. As yet, proton magnetic resonance spectroscopy (^{1}H-MRS) has not been used to study the changes occurring in myocarditis and subsequent HF. ^{1}H-MRS allows to quantify metabolites and to correlate them to heart function data obtained by magnetic resonance imaging (MRI). We aimed to explore the diagnostic potential of ^{1}H-MRS for detecting and monitoring metabolic changes in the course of myocarditis.

Methods. Myocardial function of male young Lewis rats with EAM was quantified by performing left ventricular ejection fraction (LVEF) analysis in short axis cine images covering the whole heart. Inflammatory cellular infiltrate was assessed by immunohistochemistry. Myocardial tissue was analyzed using ex-vivo proton magic angle spinning MRS (^{1}H-MAS-MRS) by placing standardized pieces of a mid ventricular short axis slice of myocardium into a 4 mm zirconium rotor and spinning at 4kHz at 293K. Water presaturation was applied to obtain the proton spectrum.

Results. Inflammation was confirmed histologically in myocarditis samples by the presence of an inflammatory cellular infiltrate and CD68 positive staining. A significant increase in the metabolic ratio of taurine/creatine (Tau/Cr) obtained by MRS was observed in myocarditis compared to healthy controls (21 d acute EAM: 4.38 (±0.23), 21 d control: 2.84 (±0.08), 35 d chronic EAM: 4.47 (±0.83) and 35 d control: 2.59 (±0.38), $P<0.001$). LVEF was reduced in diseased animals (myocarditis: 55.2% (±11.3%), control: 72.6% (±3.8%), $P<0.01$) and correlated with Tau/Cr ratio ($R=0.937$, $P<0.001$).

Conclusions. Metabolic alterations occur acutely with the development of myocarditis. Myocardial Tau/Cr ratio as detected by proton MRS is able to differentiate between healthy myocardium and myocardium from rats with EAM and correlates with functional parameters.

Abstract (deutsch):

Einleitung. Experimentelle-Autoimmun-Myokarditis (EAM) in Nagern ist ein bekanntes Tiermodell für Myokarditis und dilatierte Kardiomyopathie (DCM). Ein veränderter Stoffwechsel spielt möglicherweise eine wichtige Rolle in der Pathogenese einer DCM und einer daraus resultierenden Herzinsuffizienz. Weitere Untersuchungen des Stoffwechsels könnten sowohl neue diagnostische Informationen liefern, als auch helfen mechanistische Abläufe während einer Myokarditis und bei Herzinsuffizienz besser zu verstehen. Magnetische Resonanzspektroskopie mit Protonen (1H-MRS) wurde bisher noch nicht zur Untersuchung von Veränderungen während einer Myokarditis und der daraus folgenden Herzinsuffizienz verwendet. Unser Ziel war es Unterschiede im Kreatinmetabolismus zwischen Ratten mit EAM und gesunden Tieren zu identifizieren.

Methoden. Die Herzfunktion von jungen männlichen Lewis-Ratten mit EAM wurde durch Bestimmung der linksventrikulären Ejektionsfraktion (LVEF) in Kurzachsen Cine-Bildern quantifiziert. Inflammatorische zelluläre Infiltrate wurden durch immunhistologische Aufarbeitung von Myokardschnitten analysiert. Myokardgewebe wurde mit ex-vivo Protonen Magic Angle Spinning MRS (1H-MAS-MRS) untersucht.

Ergebnisse. Eine Myokarditis konnte histologisch durch inflammatorische Zellinfiltrate und durch ein positives CD68 in der Immunhistologie bestätigt werden. Ein signifikanter Anstieg des Metaboliten-Verhältnis von Tau/Cr (Taurin/Kreatin) konnte in den 1H-MAS-MRS Messungen in den Myokarditis-Tieren gegenüber den gesunden Kontrollen beobachtet werden (21 d acute EAM, 4.38 (±0.23); 21 d control, 2.84 (±0.08); 35 d chronic EAM, 4.47 (±0.83); 35 d control, 2.59 (±0.38); $P < 0.001$). Die LVEF war in den kranken Tieren reduziert (EAM, 55.2% (±11.3%); control, 72.6% (±3.8%); $P < 0.01$) und korrelierte mit dem Tau/Cr Verhältnis ($R = 0.937$, $P < 0.001$) der entsprechenden Ratten.

Schlussfolgerung. Metabolische Veränderungen treten bereits in der akuten Phase einer Myokarditis auf. Es konnte gezeigt werden, dass das myokardiale Verhältnis von Tau/tCr aus den 1H-MRS Messungen mit der Myokard-Funktion korreliert und zwischen Myokardgewebe aus gesunden Ratten und Tieren mit EAM unterscheiden kann.

Objectives

Despite new developments and studies, diagnosing and monitoring myocarditis remains challenging. The mechanisms of the disease are poorly understood and clinical symptoms frequently do not correlate with functional impairment. Proton magnetic resonance spectroscopy (^{1}H-MRS) can quantify metabolites and could be incorporated into protocols for magnetic resonance imaging (MRI) which assess morphology and function. As of yet ^{1}H-MRS has not been used to study the changes occurring in myocarditis and subsequent heart failure. This project investigates the metabolic changes and explores the diagnostic potential of ^{1}H-MRS in acute myocarditis and subsequent chronic cardiomyopathy. An experimental animal model of myocarditis, experimental autoimmune myocarditis (EAM) in rodents, causes significant pathological changes with high reproducibility. Ex-vivo proton magic angle spinning MRS (^{1}H-MAS-MRS) is used to provide optimal acquisition quality. The aim is to develop new pathways for the assessment of myocarditis in order to enhance the understanding of the disease mechanisms and to identify imaging- based biomarkers for diagnosis and monitoring.

Background

Myocarditis

Definition, Aetiology and Prognosis

Myocarditis is an inflammatory disease of the myocardium caused by infections, autoimmune diseases, hypersensitivity reactions, toxic drug reactions or other non-infectious triggers (Table 1). In the classification of cardiomyopathies published in 1996 by the World Health Organization (WHO), myocarditis is defined as an inflammatory disease of the heart muscle tissue and classified as a specific cardiomyopathy [1]. In 2007, the European Society of Cardiology working group on myocardial and pericardial disease defined myocarditis as inflammatory disorder of the heart with often preserved left ventricular size [2]. Despite limited sensitivity and specificity, endomyocardial biopsy (EMB) remains the invasive reference standard for diagnosing myocarditis. The main cause of myocarditis in North America and Europe is viral infection with enterovirus, adenovirus, influeza viruses, human herpes virus-6 (HHV-6), Epstein-Bar-Virus (EBV), cytomegalovirus and notably parvovirus B19 (PVB19) as demonstrated by polymerase chain reaction (PCR) after EMB. Nonviral infections such as Trypanosoma cruzi (Chagas disease), Borrelia burgdorferi (Lyme disease) and Corynebacterium diphtheriae are more common in developing countries [3] [4] [5]. Noninfectious causes include numerous medications including antibiotics (e.g. penicillins, tetracyclines), antipsychotics (e.g. clozapine) and antiphlogistics (e.g. mesalamine), which are usually reversible after withdrawal of the causative agent [6] [7]. Autoimmune diseases such as hypereosinophilic syndrome (Loeffler's disease), systemic lupus erythematosus (SLE) and Churg-Strauss syndrome as well as other systemic diseases such as sarcoidosis can also cause myocardial inflammation [8] [9] [10].

Table 1: Tabular summary of causes of myocarditis subclassified into infectious, immune-mediated and toxic etiology according to Caforio et al [11] . The most common cause of human myocarditis is thought to be viral infection.

1. Infectious myocarditis	
Bacterial	Staphylococcus, Streptococcus, Pneumococcus, Meningococcus, Gonococcus, Salmonella, Corynebacterium diphtheriae, Haemophilus influenzae, Mycobacterium tuberculosis, Mycoplasma pneumoniae, Brucella
Spirochaetal	Borrelia, Leptospira
Fungal	Aspergillus, Actinomyces, Blastomyces, Candida, Coccidioides, Cryptococcus, Histoplasma, Mucomycoses, Nocardia, Sporothrix
Protozoal	Trypanosoma cruzi, Toxoplasma gondii, Entamoeba, Leishmania
Parasitic	Trichinella spiralis, Echinococcus granulosus, Taenia solium
Rickettsial	Cociella brunetti, R. rickettsii, R. tsutsugamushi
Viral	Coxackieviruses A and B, echoviruses, polioviruses, influenza A and B viruses, respiratory syncytial virus, mumps virus, measles virus, rubella virus, hepatitis C virus, dengue virus, yellow fever virus, Chikungunya virus, Junin virus, Lassa fever virus, rabies virus, human immunodeficiency virus-1, adenoviruses, parvovirus B19, cytomegalovirus, human herpes virus-6, Epstein-Barr virus, varicella-zoster virus, herpes simplex virus, variola virus, vaccinia virus.
2 Immune-mediated myocarditis	
Allergens	Tetanus toxoid, vaccines, serum sickness, Drugs: penicillin, cefaclor, colchicine, furosemide, isoniazid, lidocaine, tetracycline, sulfonamides, phenytoin, phenylbutazone, methyldopa, thiazide diuretics, amitriptyline
Alloantigens	Heart transplant rejection
Autoantigens	Infection-negative lymphocytic, infection-negative giant cell Associated with autoimmune or immune-oriented disorders: systemic lupus erythematosus, rheumatoid arthritis, Churg-Strauss syndrome, Kawasaki's disease, inflammatory bowel disease, scleroderma, polymyositis, myasthenia gravis, insulin-dependent diabetes mellitus, thryrotoxicosis, sarcoidosis, Wegener's granulomatosis, rheumatic heart disease (rheumatic fever)
3.Toxic myocarditis	
Drugs	Amphetamines, anthracyclines, cocaine, cyclophosphamide, ethanol, fluorouracil, lithium, catecholamines, hemetine, interleukin-2, trastuzumab, clozapine
Heavy metals	Copper, iron, lead
Miscellaneous	Scorpion sting, snake and spider bites, bee and wasp stings, carbon monoxide, inhalants, phosphorus, arsenic sodium azide
Hormones	Pheochromocytoma, vitamins: beri-beri
Physical agents	Radiation, electric shock

The disease may affect patients of all ages, but it is most frequent in the young (< 40 years). Acute myocarditis resolves in 50% within 2-4 weeks, but in 25% of cases persistent cardiac dysfunction develops and 12-25% progress to dilated cardiomyopathy (DCM) and heart failure or die from sudden cardiac death [1] [11] [12] [13] [14]. In children with an identified cause of DCM, myocarditis was

documented in 46% of the cases [13]. Long-term follow-up in adult patients with acute myocarditis showed the development of DCM in over 20% of patients over three years [14]. Myocarditis is also one of the main causes of sudden cardiac death in young people as reported in studies addressing this issue, with a prevalence ranging from 2 to 42% of cases as determined by post-mortem analysis [15] [16] [17]. Overall prognosis of myocarditis however depends on its aetiology, its clinical presentation and the disease stage at time of diagnosis [12] [18] [19].

Pathogenesis

The pathophysiology of human myocarditis is not completely understood. Most studies have been conducted in murine models of enteroviral myocarditis [20]. Viral myocarditis can be differentiated into three phases, beginning with the acute phase, which only takes a few days, followed by the subacute phase, which can range from weeks to months before finally evolving into a chronic phase. The acute phase involves the entry and replication of the virus and the imminent injury to (cardio)myocytes with myocyte necrosis, exposure of intracellular antigens, edema and the initial response of the immune system with infiltration of natural killer cells and macrophages. In the subacute phase, autoimmune processes lead to additional myocardial injury due to molecular mimicry of activated virus-specific T lymphocytes [12]. Further cytokine activation and viral and (auto)-immune antibodies increase tissue damage, lead to fibrotic changes and provoke deterioration of cardiac function. Most patients' heart function recovers after elimination of the infectious or non-infectious trigger even though some fibrotic scars may remain. In some cases the autoimmune processes persist and a chronic phase develops, which is characterized by myocardial remodeling and DCM [4] [21]. In addition, genetic predisposition may play an important role for the development of myocarditis and its progression to a chronic phase and DCM [22] [23].

Diagnosis

The clinical presentation of myocarditis ranges from asymptomatic and mild symptoms of chest discomfort to ventricular arrhythmias and life-threatening

cardiogenic shock [12]. The diversity of the symptoms makes it challenging to establish the diagnosis in standard clinical settings. As yet, there is no single clinical or imaging finding that confirms the diagnosis of myocarditis with absolute certainty. The diagnosis is rather based on an integrated synopsis of clinical assessment and noninvasive test results that are associated with myocarditis: viral infection in the weeks prior to the onset of disease; new regional or global wall motion abnormalities as detected on echocardiography; ST-segment and T-wave changes, Q waves, AV block and ventricular tachycardia or fibrillation on ECG; increases in creatine kinase (CK), creatine kinase-myocardial band (CK-MB) and troponin. All of these findings have very low specificity for myocarditis and in many cases other cardiac conditions such as coronary heart disease (CAD), hereditary cardiomyopathy or valvular heart disease, have to be ruled out before the diagnosis of myocarditis can be established [11]. The reference standard for diagnosing myocarditis remains EMB with histopathology and immunohistology. Nevertheless, EMB is an invasive procedure with the potential for complications, a relatively low sensitivity due to so-called sampling error and a high inter-observer variability in interpreting biopsy specimens [24] [12]. Current guidelines recommend EMB in severe clinical scenarios and in patients with heart failure that do not include the most common presentations of myocarditis [25]. EMB in suspected myocarditis is thus not routine practice. In order to improve recognition in clinical practice, new criteria in consensus of experts are proposed for EMB in suspected myocarditis: these include the referal of patients to tertiary referral units with experience in the procedure and the validation in future multicentre registries [11].

Cardiac magnetic resonance (CMR) in myocarditis

CMR imaging has evolved as the most sensitive and valuable noninvasive tool for diagnosing myocarditis in the recent years [26] [27] [28] [29]. It is suggested to perform CMR prior to EMB in stable patients, but this does not apply in life-threatening situations [30] [31]. With CMR, various important parameters which may be altered in myocarditis can be evaluated: CMR allows the precise evaluation of the heart function, it can detect myocardial edema and pericardial effusions, and gadolinium (Gd) contrast agents can be used to detect focal myocardial injury. Initially, early gadolinium enhancement and T2 ratio were used to compare and

quantify the signal alterations between myocardial tissue versus skeletal muscle tissue. This helps to differentiate between specific patient groups, but for the individual diagnosis, these techniques may be susceptible to errors due to a significant overlap with the reference values of a healthy individual. To try to overcome some of the shortcomings of the single techniques and to combine their strengths (high specificity of LGE and good sensitivity of early Gd enhancement and T2 ratio), particular criteria have been defined by a international Consensus Group on CMR Diagnosis of Myocarditis [32]: These *Lake Louise criteria* give detailed recommendations on the indications, techniques and interpretation of CMR in myocarditis. The suggested scan protocol includes the use of the three aforementioned techniques and is considered positive for suspected clinical myocarditis when at least two of the following criteria are present [32]:

1. *Regional or global myocardial signal intensity increase in T2w edema images.*
2. *Increased global myocardial early gadolinium-enhancement ratio between myocardium and skeletal muscle in gadolinium enhanced T1w images.*
3. At least one focal lesion with non-ischemic *regional distribution in inversion recovery-prepared gadolinium-enhanced T1w images (LGE).*

It is suggested to repeat the CMR examination after 1-2 weeks if only one criterion was present or clinical symptoms suggest strong evidence for myocardial inflammation.

In a study presented in 2009, a total of 1174 patients with troponin-positive acute chest pain underwent coronary angiography. For 82 of these patients, in which CAD was excluded by X-ray angiography, additional workup including CMR and EMB was performed, showing a good correlation between CMR and EMB results in detecting myocarditis [26]. This was not the case for patients with chronic myocarditis [33].

New approaches in CMR are being developed to assess direct quantification of signal alterations in the myocardial tissue without the relative comparison to skeletal muscle. These techniques which include pT1 mapping [34] and T2 mapping [35], would make the results potentially less susceptible to measuring errors.

Clinical management and treatment

The treatment of most forms of myocarditis is based on very limited evidence and remains non-specific. In acute myocarditis, haemodynamically unstable patients may require intensive care admission: this may include respiratory support, mechanical cardio-pulmonary support, ventricular assist devices or extracorporeal membrane oxygenation (ECMO) [11]. In cases of suspected myocarditis with mild symptoms, it is recommended to clinically monitor the patient until a definite diagnosis can be established. This is due to the fact that a haemodynamically stable patient can rapidly develop cardiopulmonary emergencies like severe heart block or life-threatening arrhythmias [11]. If signs of heart failure develop, patients should be treated with angiotensin-converting enzyme inhibitors or angiotensin receptor inhibitors and beta-adrenergic blocker and diuretics if necessary in accordance with heart failure guidelines [36]. Management of arrhythmia in myocarditis should likewise be in line with current cardiology guidelines [37]. Physical activity should be strictly avoided during the acute phase of myocarditis independently of age, gender, severity of symptoms and therapy regimen [38]. For professional athletes, avoidance of physical activity is recommended until at least 6 months after the onset of the disease [39]. For non-athletes there is no such explicit recommendation but a similar period of time is regarded as reasonable. Specific therapy options in myocarditis are mainly experimental and efficacy has often not been proven. Nevertheless, immunohistochemical [40] [41] [42] and molecular biological analysis after EMB [25] as well as autoantibody serum testing is important to identify those patients in whom specific therapy may be appropriate. Such therapies include, for example, pharmacological treatment with acyclovir or ganciclovir in patients with herpes virus infection and myocarditis [43], interferon-beta therapy for elimination of enteroviral and adenoviral genomes [44], high dose intravenous immunoglobulin (IVIG) therapy in both viral and autoimmune antibody-mediated myocarditis when refractory to conventional heart failure treatment [45], and immunosuppressive therapy in virus-negative forms of myocarditis (giant cell myocarditis, autoimmune myocarditis, and others) [46]. Immunosuppression should only be started after ruling out active infection by PCR based on EMB [11].

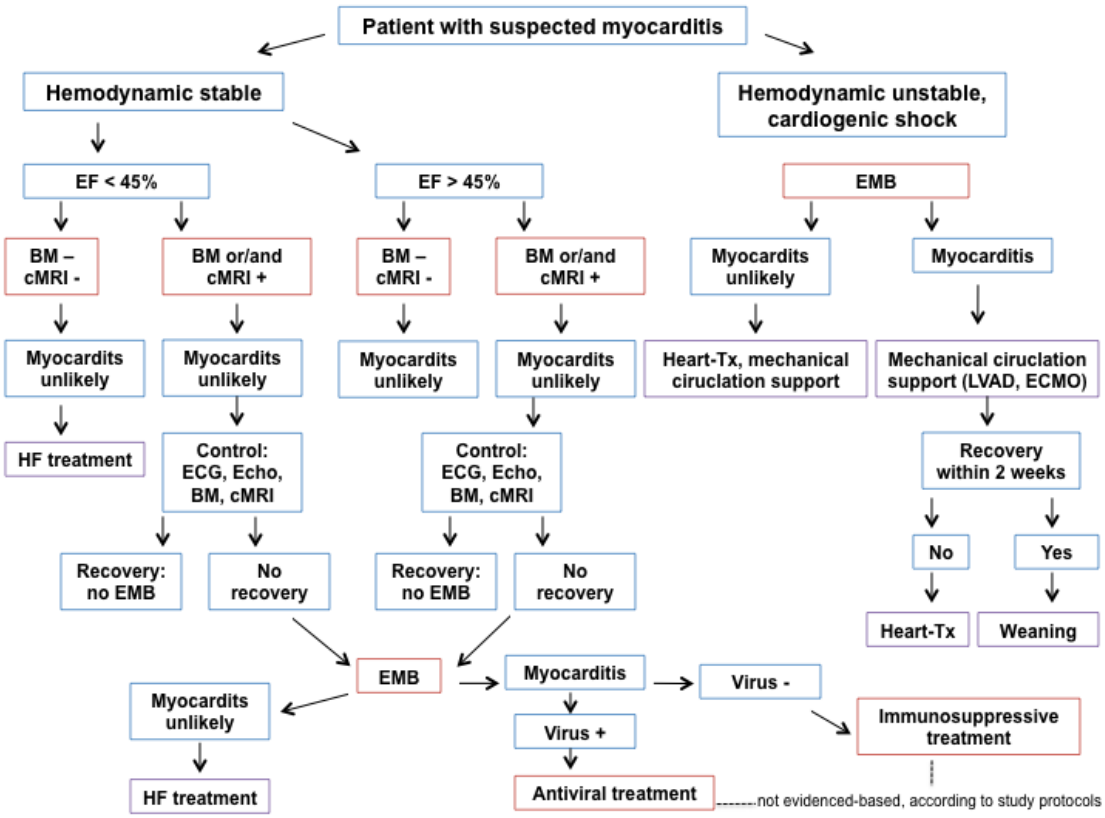

Figure 1: Possible diagnostic and therapeutic approach in patients with suspected myocarditis as proposed by Kindermann et al. [12]. Ejection fraction (EF), biomarker (BM), cardiac magnetic resonance imaging (cMRI), transplantation (Tx), ECMO (extracorporeal membrane oxygenation), LVAD (left ventricular assist device).

Myocarditis, dilated cardiomyopathy (DCM) and heart failure (HF).

Myocarditis can be a precursor of DCM, which is a form of heart failure that evidently leads to reduced quality of life and life expectancy [2] [47]. In general, heart failure is a major societal burden with a rising prevalence and is associated with increasing costs for health care systems [48]. Despite intensive research, prognosis remains poor and only small prolongation of survival has been achieved.

DCM is a clinical diagnosis. It is characterized by impaired systolic contraction and dilatation of the left ventricle (or both ventricles), which cannot be explained by coronary artery disease (CAD), abnormal loading conditions or a valvular heart disease [1] [2]. DCM can be genetic in origin, but it can also originate from toxic

substances (for example alcohol or cocaine) or from inflammatory diseases like myocarditis. The percentage of DCM that originate from myocarditis remains unknown, as to date there is no reliable tool to differentiate various forms of end-stage DCM in the absence of evident familial origin. Furthermore, it remains unclear why some cases progress towards DCM and HF over time, whereas others fully recover.

Cardiac energy metabolism

The human heart contracts about 100.000 times and cycles about 6 kg of adenosine triphosphate (ATP) every day. It generates the mechanical energy that is necessary to carry out its function by transferring chemical energy stored in fatty acids, glucose and lactate to the actin-myosin interaction of myofibrils [49].

In a first step, energy substrates (glucose, fatty acids, (lactate)) are taken up into the cardiomyocytes by specific transporters. These metabolites are further broken down in glycolysis and beta-oxidation and introduced into the Krebs cycle (Figure 2). The next step includes the respiratory chain at the inner mitochondrial membrane to produce ATP from adenosine diphosphate (ADP) – oxidative phosphorylation. In a last step, the high-energy compound ATP has to be transferred to the sites of utilization, the myofibrils. This occurs with the help of the creatine kinase (CK) system [50].

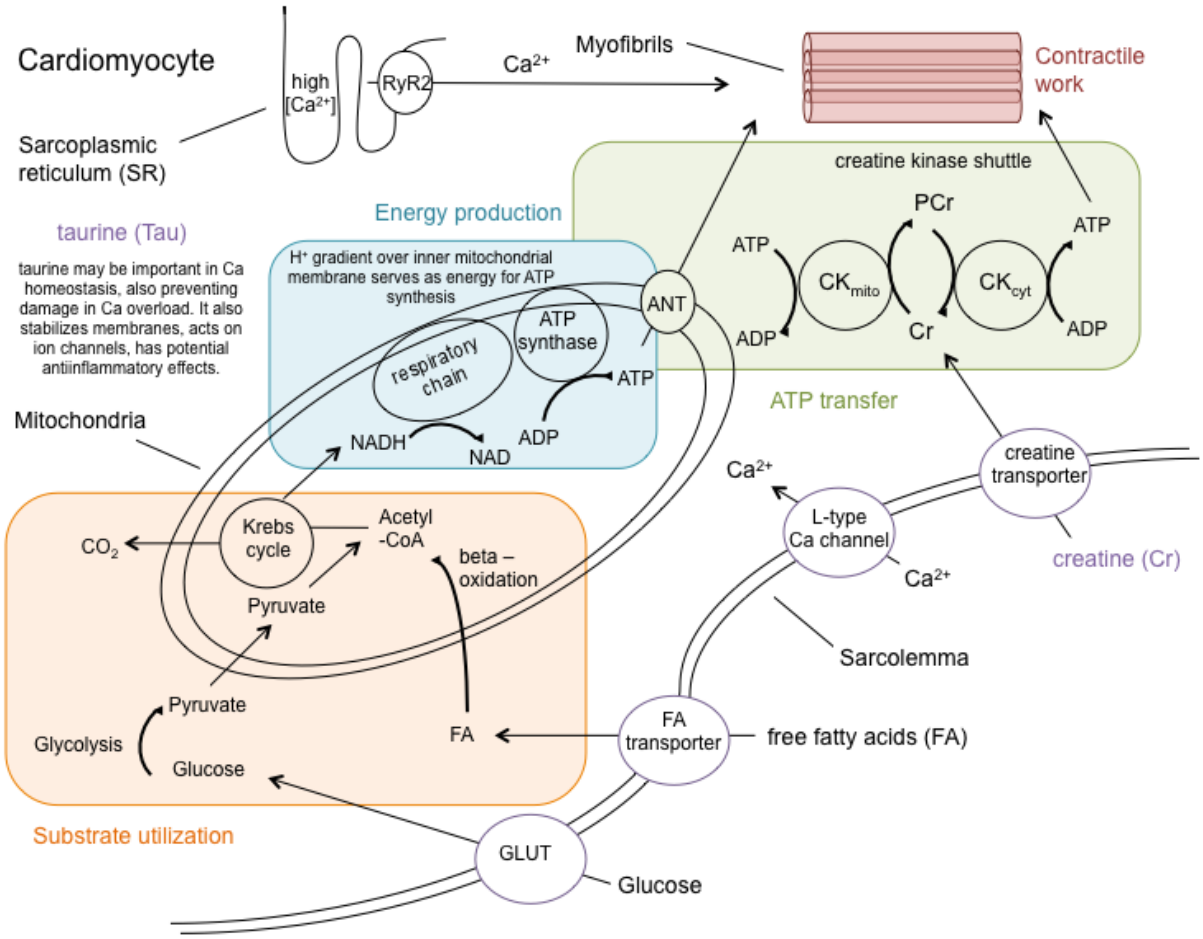

Figure 2: Simplified schematic representation of cardiac energy metabolism based on [49]. Three main components are illustrated: the substrate (glucose and free fatty acids) uptake and Krebs cycle (orange), the production of energy by oxidative phosphorylation (blue) and the transfer and utilization of energy (green). The ATP transfer from the mitochondria to the myofibrillar ATPase and other consuming reactions is mainly achieved by the creatine kinase energy shuttle and by the adenosine nucleotide translocator (ANT). Creatine, as one of the main transport metabolites for energy in the heart, is not produced in the heart but taken up by a specific plasma-membrane creatine transporter. Taurine is present in relatively high concentrations in a cardiomyocytes and various nonspecific effects have been suggested, including a protective action against myocardial infarction by reducing calcium overload in myocytes and anti-inflammatory effects [86] [88].

ATP is a large molecule that cannot easily pass the mitochondrial membrane to reach the myofibrils where its energy is needed. Therefore, ATP reacts with creatine to form phosphocreatine and ADP: phosphocreatine is a small molecule that rapidly diffuses out of the mitochondria, where the CK catalyzes the reformation of ATP and creatine. The free creatine then diffuses back into mitochondria leading to this cyclic

shuttle transfer system of high-energy bound phosphorus, which composes one very important capacity of the CK system (i). The CK system with its high energy metabolite phosphocreatine, however, also has multiple other suggested functions: (ii) most importantly it serves as immediately available energy buffer system in case of increased physical activity, (iii) it acts as spatial energy buffer, directing intracellular energy flux, (iv) it keeps cellular free ADP low and prevents a net loss of adenine nucleotides and (v) it controls local ATP/ADP ratio and thus increases the thermodynamic efficiency of ATP hydrolysis [51]. As one can see, all properties are directly associated with the correct and efficient functioning of energy supply and transport to myofibrils for contractile work in the cardiomyocytes.

Creatine is synthesized in liver and kidney and then taken up from myocytes by a specific membrane creatine transporter [52]. Usually creatine is present in myocytes as free creatine (1/3) and phosphocreatine (2/3) and one of its main functions is to act as an energy buffer. However, in cases in which energy demand surpasses energy supply, phosphocreatine levels fall. ATP concentration is kept at normal level but ADP levels still rise [53]. Increased ADP levels may then inhibit intracellular enzymes, leading to failure of the heart's contraction mechanism.

In heart failure, various other changes occur at the energy metabolism level, leading to a metabolic derangement and further functional impairment [54] [55]. This altered metabolism is thought to play an important role in the pathogenesis [53] [56] [49]. Reduced substrate uptake and utilization may lead to limited cardiac function. Studies show that fatty acid utilization is significantly decreased in advanced heart failure, whereas it is slightly increased in early heart failure [57] [58]. For glucose utilization it was shown that it may be increased in early heart failure as well, and a decline has been described during later stages of the disease [59]. Some studies have conflicting results and the interpretation of intracellular metabolism data remains difficult, as concentrations of these substances in other compartments such as plasma may be altered as well [60]. Fibrosis in heart tissue may also lead to additional difficulties with interpretation. In addition, oxidative phosphorylation can reduce cardiac function when structural abnormalities are present in mitochondria [61], activity of membrane electron transport-chain complexes is reduced [62] or the regulation mechanisms based on substrates are impaired [63]. Even if at advanced stages of heart failure, ATP levels drop by 30% - 40%, average ATP levels remain above the requirements of ATP-consuming reactions and thus do not limit contractile

function [64] [65]. The main issue is a drop of total creatine (phosphocreatine and free creatine, 30% - 70%), leading to a reduction in energy buffering capacity and ATP transfer capacity through the mitochondrial membrane [66]. This may be one of the main reasons for the loss of contractile reserve [67]: the drop of creatine is thus discussed in the energy-starvation hypothesis in the failing heart [56] [49].

As mentioned in the previous chapter, chronic myocarditis is a potential precursor for the development of DCM and thus can be accompanied by the aforementioned metabolic changes. However, very little is known about alterations of cardiac metabolism in acute myocarditis. In one experimental study in mice [68] with experimental viral myocarditis, cytosolic and mitochondrial ATP/ADP ratios, as determined by nonaqueous fractionation, were significantly altered. This was based on an antibody-mediated modulation of the function of the adenine nucleotide translocator (ANT) in the inner mitochondrial membrane of myocytes, which is a known autoantigen in myocarditis. These changes have only been observed in case of antibody-positive infection, whereas the infected but antibody-negative mice were within the control range of non-infected animals. In the same antibody-positive animals, the authors observed a decrease of creatine phosphate but an increase of free creatine.

Alterations of metabolic processes in the heart might be both source and consequence of other steps involved in the development of heart failure, including excess collagen production (myocardial fibrosis) and ventricular remodelling [49] [53] [59] [60].

Study of the cardiac metabolism may thus provide insights into the pathology of myocarditis and heart failure and may provide new diagnostic tools.

Magnetic resonance spectroscopy (MRS)

General background

Nuclear magnetic resonance (NMR) spectroscopy, in biomedicine / medicine, often also referred to as magnetic resonance spectroscopy (MRS), is a powerful method for determining the structure of organic molecules and natural compounds. In contrast to magnetic resonance imaging (MRI), which is well established in clinical applications and makes use of the strong composite signal from water protons to provide morphological information on the body, MRS detects spectral information from various nuclei of small molecules with much weaker signals and much lower concentrations. The main nuclei that have been investigated in biomedicine are protons (^{1}H), carbons (^{13}C), phosphorus (^{31}P) and to some extent nitrogen (^{15}N) that all have the spin I=1/2. The magnetic moment μ of a specific nucleus and the signal that can be obtained with it are dependent on the gyromagnetic ratio γ and the isotopic occurrence in nature (Formula 1).

$$\mu = \gamma\hbar\sqrt{I(I+1)}$$

^{1}H and ^{31}P have a high natural isotopic occurrence (99.98% and 100%, respectively) and a high γ, whereas ^{13}C and ^{15}N have low gyromagnetic ratios and are less common natural isotopes with 1.1% and 0.37%, respectively. The signals received from protons and phosphorus are therefore stronger than those of carbon and nitrogen. In general, the resonance signals of nuclei in MRS are dependent on the external magnetic field strength (B_0), the radio frequency (RF) and the extranuclear electron shielding. To be able to assign an unambiguous numerical locater to each peak, the resonance frequencies are divided by the spectrometer frequency and put into relation with a reference substance (for ^{1}H and ^{13}C tetramethylsilane (TMS)) to obtain the chemical shift. The raw data from an FT-NMR (Fourier transform NMR) experiment are the free induction decay (FID) of all nuclei in their different chemical environments. This information in the time domain can be transferred into the frequency domain with Fourier's transformation. These results are then presented in

the well-known chemical shift spectra with parts per million (ppm) as ‘unity’ due to the fact that the frequency differences between nuclei (in Hz) have been divided by the spectrometer frequency (in MHz). The difference in chemical shift of nuclei of the same type (for example protons) then results from the different chemical environments in the molecules e.g. adjacent functional groups, direct binding partners, solvent etc. The chemical environment has a direct effect on the electron shielding and leads to an observable chemical shift. Interpretation of the chemical shift then gives information about the chemical structure of a molecule.

In a mixture of metabolites, it is possible to obtain information about ratios and concentrations from MRS experiments, as the area under the peak in the MRS spectrum is directly proportional to the concentration of a specific metabolite. Molecules with high concentrations have therefore peaks of high amplitude compared to substances at low concentration. For absolute quantification, an external standard in a known concentration may be added (e.g. TMS).

Unlike other imaging modalities such as positron electron tomography (PET) and single-photon emission computer tomography (SPECT), MRS inherently provides information about metabolites without the use of ionising radiation and without requiring the administration of external tracers and contrast agents. Proton MRS is a non-invasive, non-destructive and non-radiation technique that, among others, allows to quantify myocardial metabolites such as creatine, taurine, and lipids [69] [70]. As it is based on the same basic physical principles as MRI, it may be used on the same equipment, which makes it a potential candidate for use in clinical applications.

^{1}H-MAS-MRS

Proton magic angle spinning magnetic resonance spectroscopy (^{1}H-MAS-MRS) is a method used mainly in materials science and protein biology for spectral analysis of non-liquid samples [71]. It has excellent spectral resolution and can be used to analyze ex-vivo samples of a variety of tissues [72] [73], where it is often referred to as high resolution MAS-MRS (HR-MAS-MRS). It combines techniques from both solid-state and classical liquid NMR, as classical solution state pulse sequences are

used but the sample is spun at the magic angle as in solid-state NMR. In liquid state NMR, molecules at temperatures not close to 0 K have no motional restrictions and move and rotate faster than the NMR observation frequency. This leads to an averaging in molecular orientation and results in narrow spectral lines. This averaging does not apply to non-liquid samples and molecular interactions such as dipolar coupling, chemical shift anisotropy and quadrupolar coupling result in spectral broadening in NMR experiments. However, dipolar interaction and chemical shift anisotropy have an angular dependence ($3*\cos^2\theta-1$), which can be used to undo their effect. If θ, which is the angle between the static magnetic field and the internuclear vector of the interaction, is θ=54.7° the equation $3*\cos^2\theta-1 = 0$ is satisfied (Figure 4). Rotating at high rates at this particular angle leads to significant reduction of interactions and spectral line broadening. The dipolar coupling then averages to zero, the chemical shift anisotropy averages to a non-zero value and the quadrupolar interaction is partially reduced as well. The angle θ=54.7° is therefore called the magic angle as MAS mimicks the time-averaged molecular motion in liquid samples.

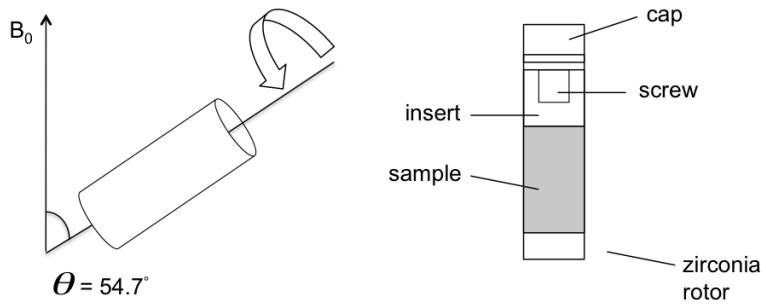

Figure 3 [74]: Schematic representation of the magic angle spinning and the angle θ=54.7° (left) and a MAS rotor with cylindrical sample space, insert (also called spacer), insert screw and cap. Most MAS rotors are made of zirconium and have a diameter of 3.2 mm or 4 mm.

Usually, 10-50 mg of tissue is required to perform ex-vivo MAS-MRS experiments. The spectrometers for these ex-vivo experiments have magnetic fields up to 21.2 T (900 MHz), which are very high compared to the standard clinical MR systems with 1.5 T (64 MHz) and 3 T (128 MHz) for in-vivo experiments (in specific scientific centres, clinical MR systems with 7 T are available). Therefore, the resolution is better in ex-vivo experiments, which makes them suitable for identifying target

metabolites before planning in-vivo studies. Furthermore, sample preparation is relatively easy and quick to perform which makes ^{1}H-MAS-MRS an ideal method for the study of intact tissue.

Use in metabolomics

Metabolomics is a systematic approach to profile low molecular weight metabolites in tissue and cells. The information that is gathered arises downstream of transcription and translation and may therefore be a better indicator of enzyme activity than the determination of mRNA or other gene activity markers [75]. The results are complementary to histopathology and immunohistochemistry as they permit biochemical composition to be related to quantitative histopathologic findings from the same tissue. The techniques used for metabolic analysis include high-pressure liquid chromatography (HPLC), gas chromatography (GC), mass spectroscopy (MS), and NMR spectroscopy. These methods all use tissue or tissue extracts for the analysis, which means that they are ex-vivo techniques (apart from in-vivo NMR). Chromatography and MS have very high sensitivity and reproducibility but require a more complicated sample preparation, which includes using media that are in the liquid or gas phase. In NMR on the other hand, ex-vivo experiments can be performed on aqueous extracts from tissue or on unaltered whole tissue samples directly.

Various tissues and tumors have been investigated with HR-MAS-MRS. Martinez-Bisbal et al. [76] investigated biopsy samples (and aqueous chemical extracts) of human high-grade gliomas with ex-vivo HR-MAS spectroscopy and conducted a detailed assignment of the biochemical compounds. Wilson et al. [77] compared the metabolite signals in ex-vivo HR-MAS-MRS to the in-vivo results in childhood brain tumors, suggesting that the main source of correlation errors was based on low signal-to-noise ratio in in-vivo measurements. Millis et al. [78] classified human liposarcoma and lipoma using ex-vivo HR-MAS spectroscopy and correlated their results with histological findings. Varma et al. [79] performed ex-vivo MRS on colonic mucosal samples of an animal inflammatory bowel disease model and showed that it is possible to differentiate diseased tissue from healthy tissue. Sitter et al. [80] compared the spectroscopic profiles of breast cancer tissue in 85 patients with non-

involved tissue and clinical parameters using ex-vivo HR-MAS-MRS. Chan et al. [81] investigated the MAS spectra of specimens of human colorectal cancer and compared their metabolic profile with normal mucosae tissue, identifying a set of metabolites, which had different concentrations in the affected tissue. Tessem et al. [82] used proton HR-MAS spectroscopy to analyze lactate and alanine as metabolic markers in prostate cancer tissue acquired by transrectal ultrasound-guided biopsy in 98 patients. They found low concentrations of lactate and alanine in benign prostate biopsy tissue, whereas in prostate cancer tissue the concentrations were significantly higher.

Studies of in-vivo MRS have the advantage that there is no need for sample preparation and thus no procedure-induced alteration of the investigated tissue. On the other hand, in-vivo MRS has much lower spectral resolution than in-vitro MRS, and subtle changes in affected tissues may be overlooked without previous knowledge from ex-vivo experiments. For in-vivo MRS, the choice of the location of the voxel (volume pixel) is very important and should include the tissue of interest in at least 50% of the volume. This means for example that for brain tumors, at least 50% of the voxel should be tumorous tissue if one does not want to miss differences in the altered spectrum.

MRS is not very well integrated into clinical routine and diagnosis. However, MRS, in combination with other clinical results such as blood tests, tumor markers, and morphological information from imaging, might be of help in clinical situations.

In neurology for example, MRS can be applied for specific indications in neurometabolic disorders such as adrenoleukodystrophy, Canavan's disease, Alzheimer's disease, and human immunodeficiency virus dementia [83]. It has been stated that in these conditions there is an added value of MRS when MRI is positive; there is a unique decision-making information in MRS when MRI is negative; and MRS provides useful information in regard of neurologic therapeutics. ^{31}P-MRS can be integrated into a clinical protocol for tumor grading, as it is able to separate and quantify relatively the metabolites of phosphocholine and glycerophosphocholine, which have opposite associations with tumor grade [84].

As more 3 T and higher MR systems are installed in clinical institutions and pulse techniques and post-processing tools get optimized [85], MRS may develop a more widespread role in clinical protocols.

MRS is thus a non-invasive tool for the analysis of chemical tissue composition and metabolomics in disease processes. It can be used in biomedical research to study disease processes and conduct metabolic profiling, and may be used as an add-on diagnostic tool for specific indications.

Our main peaks of interest in our ex-vivo experiments were creatine, taurine and lipids. They are the most abundant small-molecule metabolites in the myocardium and can thus be detected quantitatively in future in-vivo experiments. Taurine is a sulfur amino acid with high concentration in the myocardium [86]. Various effects have been attributed to taurine, including a protective action against myocardial infarction by reducing calcium overload in myocytes [87] and anti-inflammatory effects [88].

Experimental autoimmune myocarditis (EAM)

As diagnostic workup of myocarditis remains controversial and challenging, there is a need for reliable animal models that can be used to validate existing and test novel diagnostic methods. Experimental autoimmune myocarditis (EAM) in rodents mimics human myocarditis in the acute and chronic phases [89] [90] [91] and may thus be used for the development and testing of diagnostic tools. Different protocols have been used to induce EAM in rats by immunization with cardiac myosin, using various application sites and doses. All protocols use Lewis rats, which are reported to be the only rat strain susceptible to EAM induction [89] [92] [93]. In previous research projects, our group has established an optimized immunization protocol to induce a strong and reproducible inflammatory reaction of the myocardium, which has been confirmed by immunohistochemistry analysis [94].

The assessment of myocarditis and its course of inflammatory activity over time remain challenging. New diagnostic tools are required to facilitate diagnosis and

monitoring of myocarditis. ^{1}H-MRS is able to provide in-vivo information that is not accessible with other non-invasive diagnostic tools. We therefore aimed to study the metabolic changes occurring in an animal model of experimental autoimmune myocarditis (EAM) using ^{1}H-MAS-MRS in order to identify potential targets for in-vivo ^{1}H-MRS in human myocarditis.

Materials and Methods

Animals

Young male (if not stated otherwise) Lewis rats (Janvier, Le Genest-St-Isle, France) weighing 200-280 grams were used (n=41). The rats were housed in a specific pathogen-free barrier under standardized conditions with controlled temperature and humidity on a 12 hours light / 12 hours dark cycle in groups of four or five with access to food and water *ad libitum*. All procedures and experimental protocols were performed in accordance with the *Guide for the Care and Use of Laboratory Animals* published by the US National Institutes of Health, and were approved by the Landesamt für Gesundheit und Soziales in Berlin, Germany (http://www.berlin.de/lageso; Reg 0276/11, 19.12.2011; T 0190/11, 16.05.2013).

Study protocol

Animals were randomly assigned to four study groups: (A) 21 d acute EAM (n=10), (B) 21 d control (n=7), (C) 35 d chronic EAM (n=10) and (D) 35 d control (n=8). Animals of EAM groups were immunized on day 0 and experiments (CMR (only groups (C) and (D)), MRS, histology, immunohistochemistry) were conducted in the course of the disease on day 21 for acute phase EAM and day 35 for chronic EAM (Figure 5). Preliminary experiments had shown histologically that the inflammation was most acute at day 21 (highest amount of inflammatory infiltrate) and had developed into chronic stage at day 35 (high amount of collagen (fibrosis), no more inflammatory infiltrate).

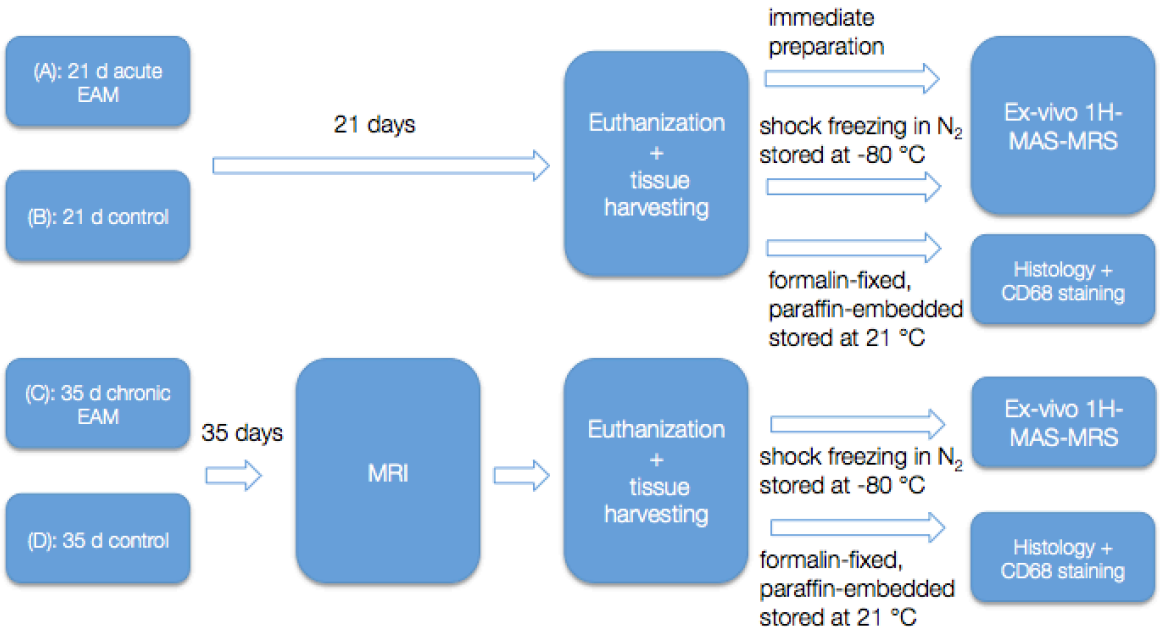

Figure 4: Study protocol with animals assigned to groups (A) 21 d acute EAM (n=10), (B) 21 d control (n=7), (C) 35 d chronic EAM (n=10) and (D) 35 d control (n=8). To investigate the effects of shock freezing (which enables temporary storage of samples and subsequent batch examination on MRS) animals of groups A and B were examined in a *fresh* stage (21 d acute EAM-fresh, 21 d control-fresh) before shock-freezing. Samples for histology and immunohistochemistry were collected and stored for all groups.

Immunization

Myocarditis was provoked by a cross immune reaction between porcine myocardial myosin and the myocardium of the rats. We used an EAM model, in which animals were immunized by injection of a suspension containing porcine myocardial myosin and Freund's adjuvant into each rear footpad [89]. The immunization was performed using an optimized protocol developed by our group [94]: The rats were immunized with a suspension containing porcine myocardial myosin (2.5 mg myosin in 1 ml suspension). To prepare 4 ml of suspension, 0.5 ml phosphate-buffered solution with 1.05 ml calcium-activated myosin from porcine heart (9.5 mg ml^{-1} in 50% glycerol, Sigma-Aldrich, Munich, Germany) was first mixed in a tube. Then, in a separate tube, 2.0 ml of complete Freund's adjuvant (Sigma-Aldrich, Munich, Germany) was mixed with 20 mg of solid *Mycobacterium tuberculosis H37 RA* (DIFCO LABORATORIES, Detroit, MI, USA). The suspensions from both tubes were then mixed, vortexed and transferred to a 10 ml record syringe (FORTUNA OPTIMA 10-

ml record syringe), which was then connected through a three-way connector (Discofix) to an empty syringe of the same type. Air bubbles were then expelled to exclude air from the suspension. The suspension was homogenized by moving the content back and forth between the two syringes for 10 min. The homogeneity of the suspension was confirmed by a drop of water on the top of that did not disperse [92]. The suspension was drawn into 1-ml sterile syringe with Luer-Lock tip and connected to a 26 G needle. The suspension was prepared freshly on the day of immunization. The rats were then immunized with 0.125 mg myosin (0.05 ml of suspension) to each rear footpad.

Cardiac magnetic resonance (CMR)

To assess cardiac function *in vivo*, rats were examined using ECG-triggered CMR imaging on a 3 T clinical MR system (Ingenia, Philips Healthcare, Best, The Netherlands) with a dedicated 70 mm solenoid small animal coil under isoflurane anaesthesia (2-3% in oxygen 1 L min^{-1}). Animals were positioned headfirst, supine, breathing freely throughout the entire imaging procedure. ECG electrodes were placed on the rat's paws. Long axis (2-chamber and 4-chamber) and a stack of short axis (seven slices) cine images were acquired to assess the following parameters using cmr42 software (version 3.4.1, Circle Cardiovascular Imaging Inc., Calgary, Canada): left ventricular ejection fraction (LVEF) and left ventricular end-diastolic volume (LVEDV).

Ex-vivo sample collection

Before MRS experiments (groups A, B) and directly after the CMR examination (groups C, D) animals were euthanized through an overdose of isoflurane and the heart was explanted by thoracotomy. It was rinsed with freshly prepared phosphate buffered saline (PBS) to remove blood. The heart was dried with paper towels and placed into a specific metal block to be cut into four equal transverse slices of the ventricular myocardium without the atria. A mid ventricular slice was stored in formalin (4%) for histological analysis. The remaining tissue slices were used for ex-vivo MRS experiments: samples were put into Eppendorf tubes, shock frozen in liquid nitrogen and stored at –80°C. To investigate the effects of shock freezing

(which enables temporary storage of samples and subsequent batch examination on MRS), animals of groups A and B were examined in a *fresh* stage (21 d acute EAM-fresh, 21 d control-fresh) before shock freezing. *Fresh* implies that the ex-vivo MRS experiments were conducted immediately after the death of the animals (< 5 min).

Magnetic resonance spectroscopy (MRS)

Shock-frozen samples were taken out of the freezer (-80°C) and allowed to warm on air (2 min). The remaining procedure is similar for frozen and fresh samples. Using a surgical scalpel, the myocardial sample (35-45 mg) was cut out of the heart slice avoiding epicardial tissue. The sample was placed into a 4 mm zirconium rotor, a spacer (insert + screw) was placed into the rotor to avoid displacement of the sample during acquisition, and the rotor was closed with a cap for the measurement [74] (Figure 6.B).

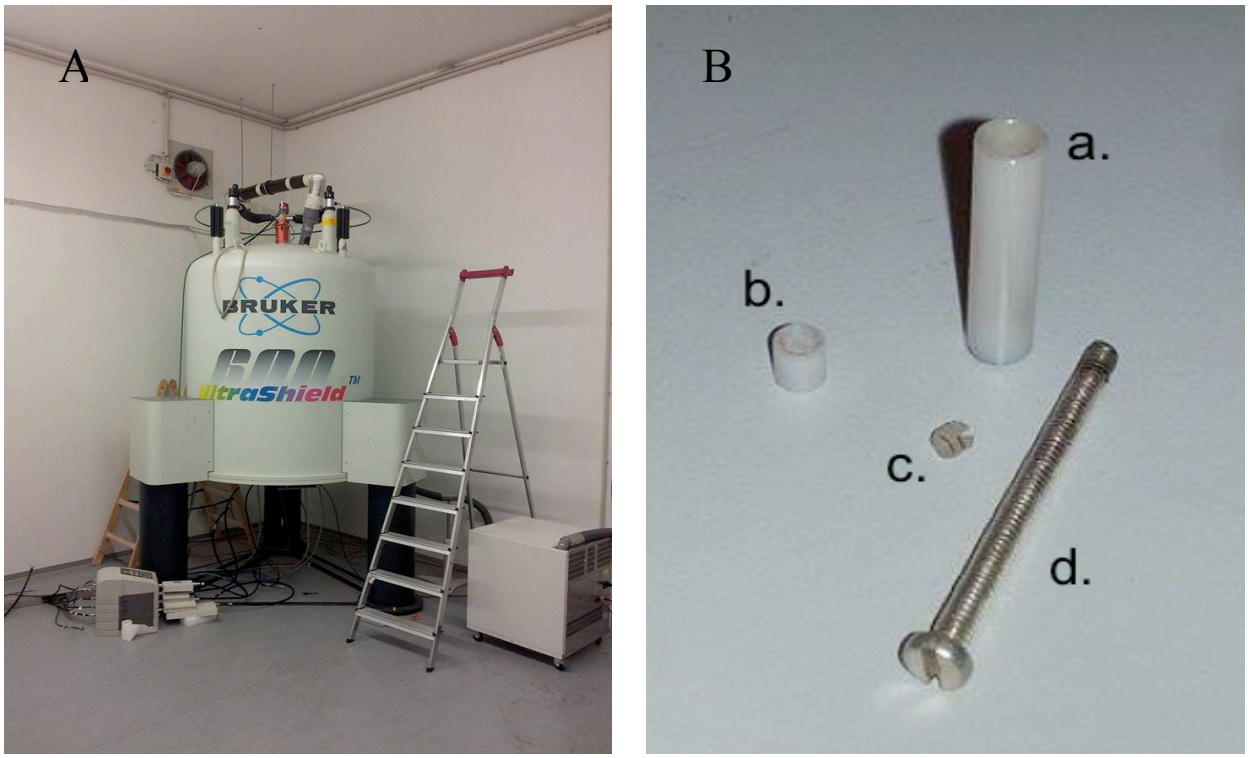

Figure 5: (A): Bruker 600 MHz (14.1 T) spectrometer equipped with Bruker BL4 MAS probe head. Samples are introduced vertically into the spectrometer (B): 4 mm zirconium rotor (a.) with spacer (b.), spacer-screw (c.), and screw to insert the spacer into the rotor (d.). Closure of the sample is achieved by use of a cap (not shown on the picture).

Putting the rotor with the sample into a centrifuge helped packing the sample more homogeneously. All experiments were performed on a 600 MHz spectrometer (Bruker BioSpin GmbH, Rheinstetten, Germany) equipped with a Bruker BL4 MAS probe head at 293 K and at a MAS frequency of 4 kHz (Figure 6.A). Water in the sample was presaturated with a low-power pulse (47 dB). The proton nutation frequency was 5000 Hz at 2.4 dB. For each experiment, 128 scans were acquired with 79988 points in a spectral width of 167 ppm (measurement time of 7 min). The spectral ^{1}H width was set to 100 kHz, which corresponds to 167 ppm on a 600 MHz spectrometer. The 31P nutation frequency was 35714 Hz at 5.00 dB. For each experiment, 128 scans were acquired with a time domain of 14590 points in a spectral width of 412 ppm. The relaxation delay was 5.00 s. All data were processed using Bruker Topspin (Bruker BioSpin GmbH, Rheinstetten, Germany) and iNMR (version 5.3, Mestrelab Research, Santiago de Compostela, Spain) software. Spectra were phased and the lactate doublet at 1.330 ppm was used as internal chemical shift reference [95]. Phase correction of zero order and first order, and baseline correction using polynomial fit to the regions of interest was applied before integration. Ratios for relative quantification were obtained by calculating the area under the peak. Ratio was either calculated between two peaks of interest directly (e.g. creatine, taurine) or by dividing the area of the peak of interest through the entire spectral region from 0.6 ppm – 4.2 ppm to avoid artifacts created by suppression of the water peak at 4.6 ppm. In samples with external standard TSP (3-(trimethylsilyl)propionic-2,2,3,3-d_4 acid sodium salt, 98%, Sigma-Aldrich, Munich, Germany), chemical shift was referenced to TSP. Using fixed amounts of standard solution (5 μl of a solution of 100 mg TSP in 2 ml of distilled water), experiments were conducted to test if TSP could be used as an external standard for absolute quantification of metabolites.

Histological and immunohistochemical analysis

Samples for the immunohistochemical analysis were obtained from the freshly explanted rat heart and fixed in formalin (4%). The formalin-fixed myocardium was

embedded in paraffin and stored at 21 °C. Macrophage infiltration of the myocardium was determined by immunohistochemical staining of CD68 from formalin-fixed paraffin-embedded cardiac tissue sections (Mouse Monoclonal antibody to CD68, Gene-Tex, Irvine, CA, USA; Secondary antibody from Bond-Max-Kit, Post Primary AL rabbit-anti-mouse IgG: Polymer Ap anti-rabbit-poly-Ap-IgG, Leica Biosystems Nussloch GmbH, Nussloch, Germany). All myocardial examinations were quantified by automated delineation through the microscope analysis software (Keyence BZ 9000+ analysis software, Itasca, IL, USA).

Statistical analysis

Statistical analysis was performed using the SPSS statistical programm (version 11.0, SPSS Inc., Chicago, IL, USA). All values were expressed as the mean ± standard deviation. Differences between groups were evaluated using the one-way ANOVA test and $P<0.05$ was considered to indicate a statistically significant difference (*= $P<0.05$, **= $P<0.01$, ***= $P<0.001$). Correlation analysis was conducted using two-tailed Pearson correlation coefficient with linear regression. Reliability of the spectral analysis was tested with two-way random single measure intraclass correlation (ICC) based on *absolute agreement*.

Results

General evaluation of ex-vivo ^{1}H-MAS-MRS in rat heart samples

Reproducibility and resolution.

MRS measurements were reproducible in all acquired samples. Nineteen out of 22 different peaks in the spectrum could be assigned based on the previously published spectral data from human skeletal muscle and rat heart muscle (Figure 7) [96] [97]. Doubts arose regarding the peak number 14, which might either be caused by carnitine or phosphocholine. The two other peaks that could not be assigned (peak 6 and peak 21) are small peaks and may be attributed to lipids or non-carbon-bound hydrogens. The resolution was comparable to the spectra of heart muscle and skeletal muscle tissue published in recent years [96] [97]. Importantly, the resolution obtained allowed relevant multiplets such as the two taurine triplets, the lactate doublet and the alanine doublet to be detected (Figure 8).

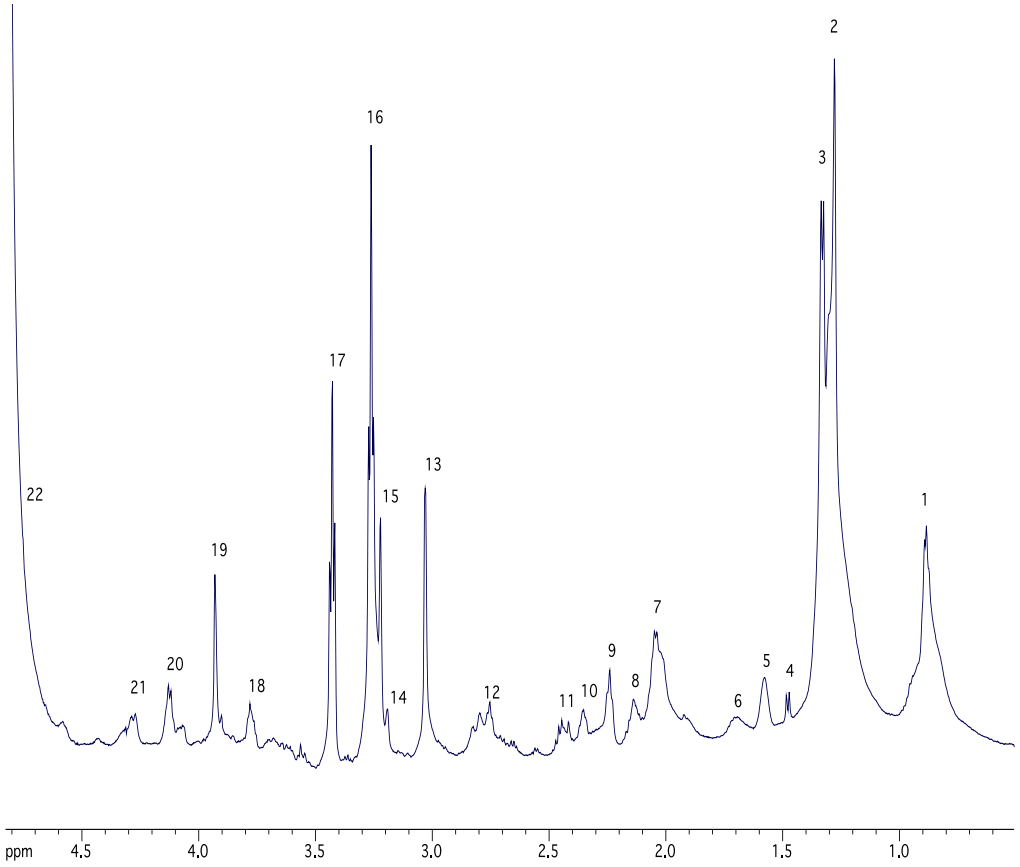

Figure 6: ^{1}H-MAS-MRS spectrum of a freshly excized healthy rat heart sample (5 min after cardiac arrest). (1) lipids ($-CH_3$), 0.89 ppm; (2) lipids $(-CH_2-)_n$, 1.28 ppm; (3) lactate ($-CH_3$), 1.33 ppm, d (reference); (4) alanine ($-CH_3$), 1.47 ppm, d; (5) lipids, 1.58 ppm; (7) lipids, 2.04 ppm; (8) glutamine (β-CH_3), 2.14 ppm; (9) lipids, 2.24 ppm; (10) glutamate (γ-CH_3), 2.35 ppm; (11) glutamine (γ-CH_3), 2.45 ppm; (12) lipids, 2.75 ppm; (13) creatine ($-CH_3$), 3.03 ppm, s; (14) carnitine/(or phosphocholine) 3.19 ppm; (15) choline (N-CH_3), 3.22 ppm, s; (16) taurine (S-CH_3), 3.26 ppm, t; (17) taurine (N-CH_3), 3.48 ppm, t; (18) alanine (-CH), 3.78 ppm; (19) creatine ($-CH_2$), 3.39 ppm; (20) lactate (-CH), 4.13 ppm; (22) water, 4.8 ppm; (6), (21) not assigned [96][97].

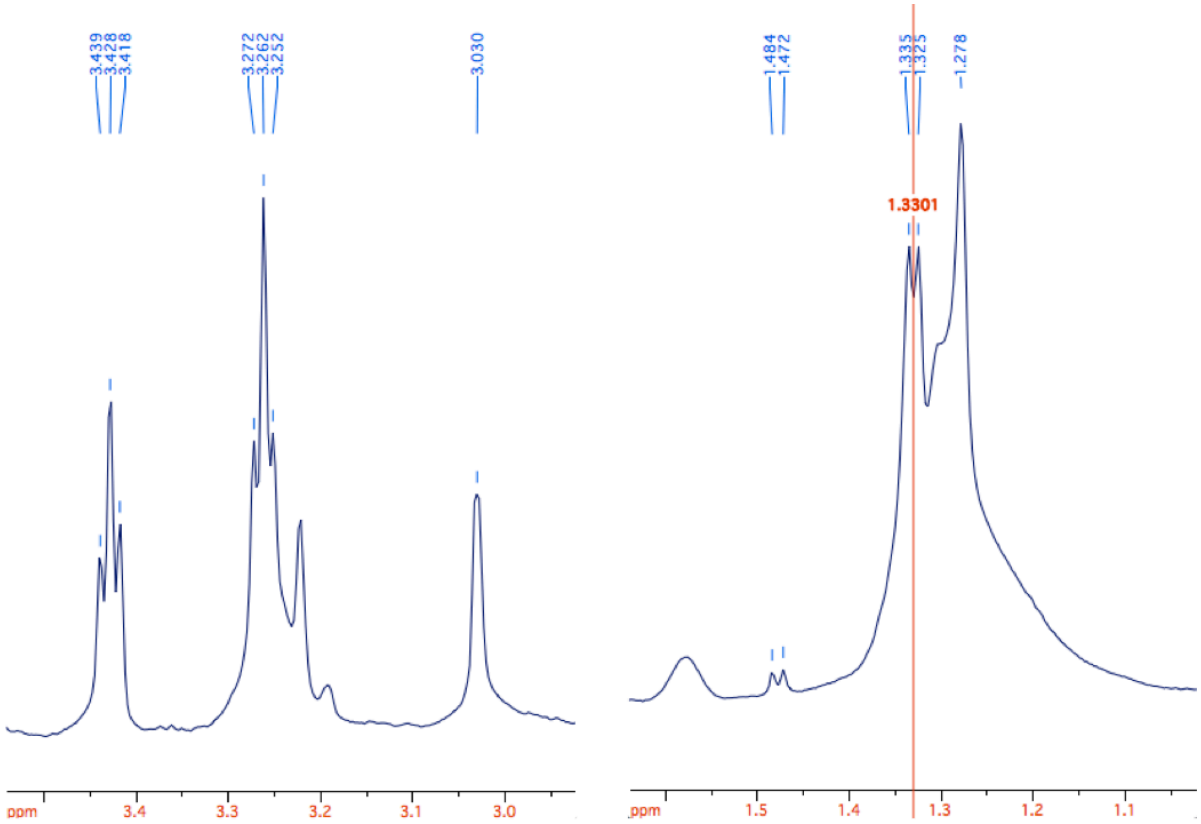

Figure 7: Fresh control sample with spectral area of taurine and creatine (2.9 ppm – 3.5 ppm) (left) and spectral area of the methylene peak, lactate and alanine (1.0 ppm – 1.6 ppm) (right) showing the excellent resolution obtained in the experiments. The two taurine triplets, the lactate doublet and the alanine doublet are well resolved. The lactate doublet was used as internal chemical shift reference (right) [95].

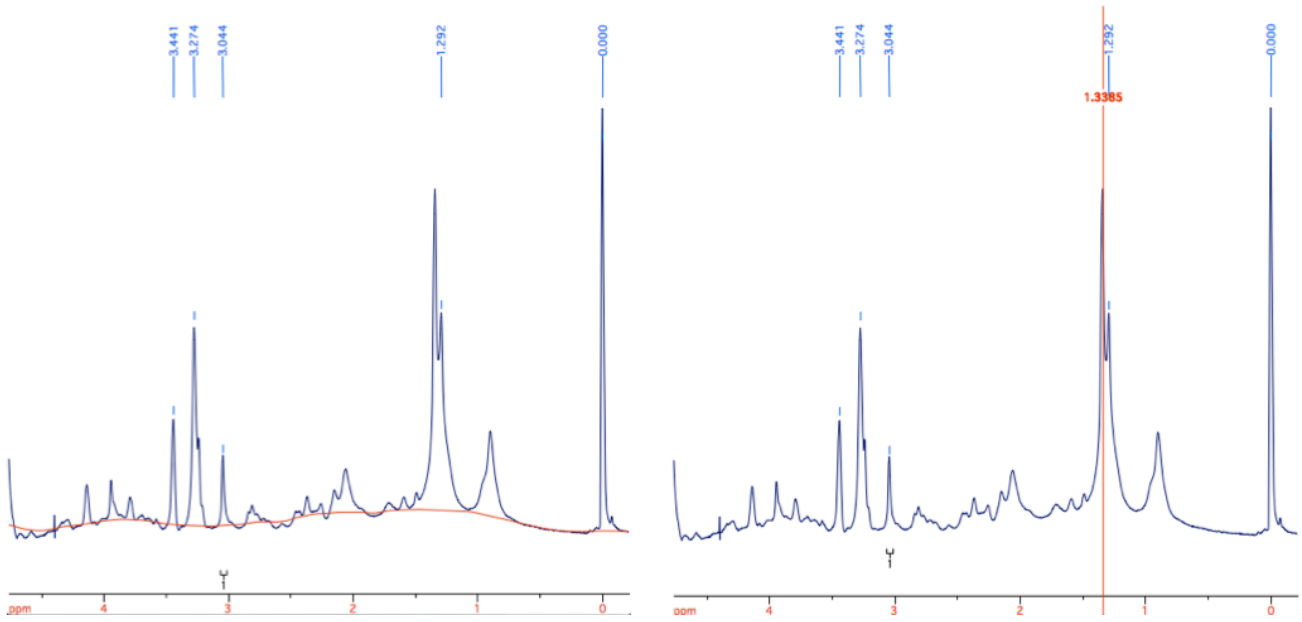

Figure 8: Whole spectrum of frozen control sample with adjusted baseline correction (right) and chemical shift reference (left). The baseline is used for calculating the integrals and thus for the quantitative analysis: Phase correction of zero order and first order is done first and baseline correction is conducted using polynomial fit to the regions of interest. The lactate doublet (1.33 ppm) was used as an internal chemical shift reference in all samples compared to the external reference TSP (0.00 ppm), which was used for verification experiments.

Additional experiments with an external standard (TSP) were conducted to evaluate if quantitative analysis of metabolites would be possible. TSP is used in NMR spectroscopy with water samples, however in our case, the samples were not liquid but solid samples. Once an appropriate concentration of TSP was found, we repeated the MRS measurement with the same prepared sample three times in a row (at 0 min, after 8 min, and after 16 min) without taking the rotor with the sample out of the spectrometer (Figure 10).

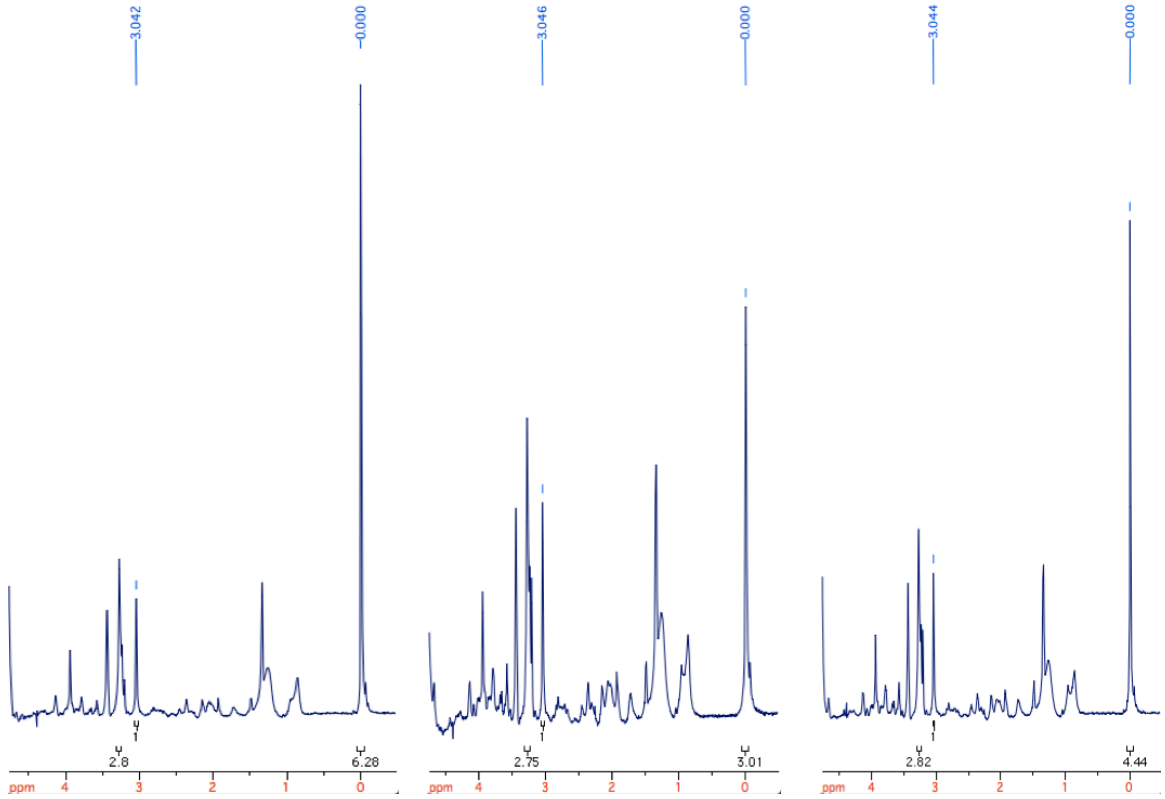

Figure 9: Full spectrum results of three repeated measurements from the same prepared frozen control sample with TSP as external standard. This sample was measured three times in a row to test if the use of TSP (0.00 ppm) as an external quantitative standard could be helpful in this application, which was not the case: the ratio of Tau/Cr was very stable with values of 2.80 / 2.75 / 2.82 whereas the ratio of TSP/creatine varied extremely with values 6.28 / 3.01 / 4.44.

We observed that the ratio of taurine/creatine (Tau/Cr) was very stable with values of 2.80 / 2.75 / 2.82, whereas the ratio of TSP/creatine was not consistent and varied extremely with values 6.28 / 3.01 / 4.44. Therefore therefore not use TSP for quantitative purposes in our samples. The water peak is often used as internal standard in in-vivo experiments [98]. However, the interstitial edema, which was confirmed histologically in the myocarditis animals, may intrinsically change the water content of a sample, rendering this approach unreliable for gaining more information on ratios of metabolites.

Inter-observer agreement of the spectral analysis was tested with intraclass correlation (ICC). 10 spectra of randomly assigned study groups were analyzed by a second observer and the Tau/Cr ratio was calculated, leading to an ICC=0.942

(P<0.001), indicating a highly reproducible analysis method. This ICC is based on schrieblesque *absolute agreement* meaning that all observers had the same previously discussed criteria for data analysis.

Freezing effect

In order to assess the effect of shock freezing on the samples (which was necessary to allow for storage of the samples after MRI and batch examination on MRS), 1H-MAS-MRS spectra of shock frozen samples were compared to freshly prepared samples (< 5 min). It was observed that freezing of the samples by shock freezing in liquid nitrogen and storing at – 80 °C led to changes in the 1H-MAS-MRS spectra (Figure 11). The difference could be best seen in the methylene peak at 1.28 ppm and this peak was used for quantifying the difference.

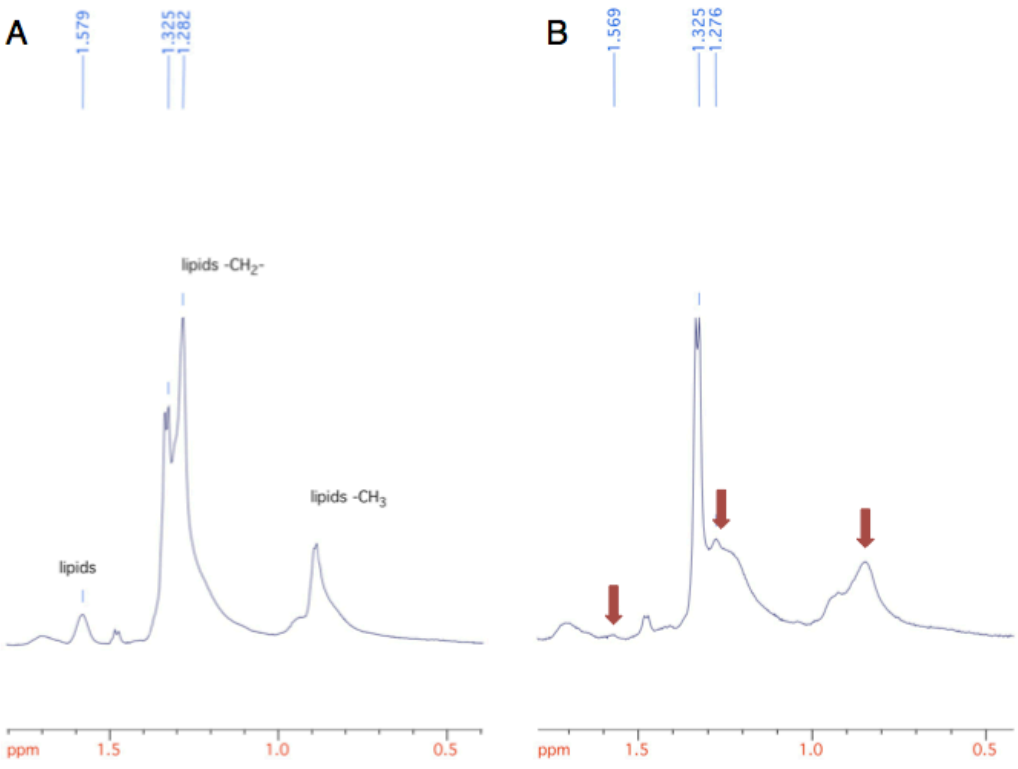

Figure 10: Part of ex-vivo ^{1}H-MAS-MRS spectrum (0.4 ppm – 1.8 ppm) of fresh (A) and 1 day frozen (B) samples of healthy rat myocardium. Characteristic lipid peaks show morphologic changes in the spectrum after shock-freezing in liquid nitrogen. The difference is best seen in the methylene peak at 1.28 ppm. The changes may be related to lipid degradation in freezing as previously described in

other tissues e.g. from rat kidneys [99]. Relative integral was calculated by dividing the area of the peak of interest (methylene) by the entire spectral region from 0.6 ppm to 4.2 ppm to avoid artifacts created by suppression of the water peak at 4.6 ppm.

The relative quantification of lipid peaks of fresh samples yields different results from those of frozen ones (Figure 12). The effect of shock freezing on the important spectral region of taurine and creatine was investigated using the Tau/Cr ratio in controls and in myocarditis animals. There was no significant different in this ratio when comparing fresh with previously shock-frozen myocardium (21 d control-fresh: 2.59 (±0.09), 21 d control: 2.84 (±0.08), 21 d acute EAM-fresh 4.14 (±0.32), 21 d acute EAM: 4.38 (±0.23); $p>0.05$). This leads to the assumption that only lipids degrade during the shock freezing procedure, whereas the other metabolites seem not to be affected. The lipid peaks also show morphologic changes (Figure 11: methyl and methylene peaks), which mainly result in broader peaks after shock-freezing. Similar changes of lipid peaks have been described in the literature for other tissues [99]. Multiplets of peaks in the spectrum that were well identifiable in the fresh sample measurements were not completely resolved in frozen spectra.

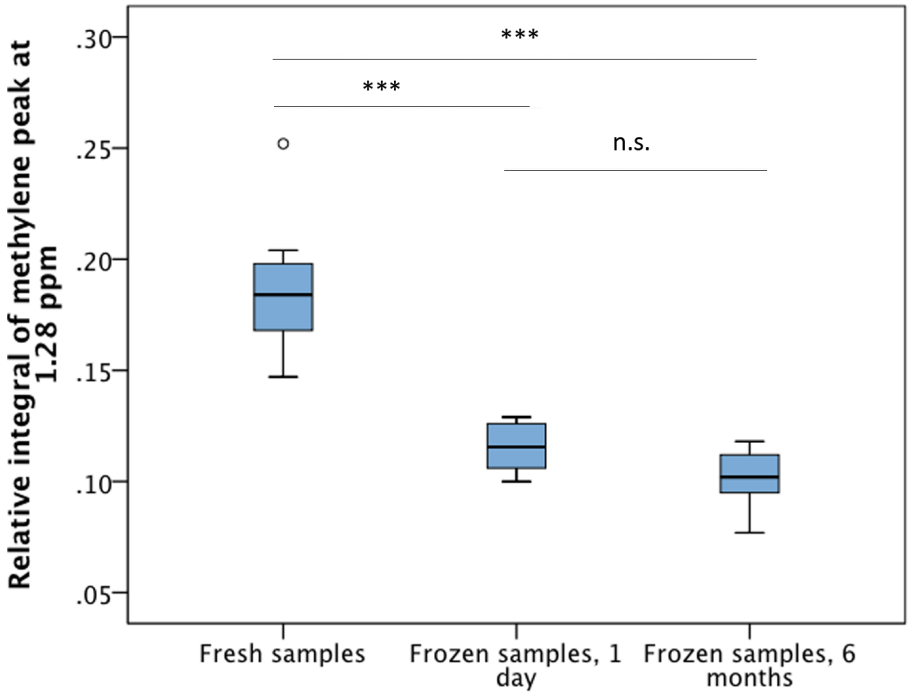

Figure 11: Comparison of relative integral of methylene peak at 1.28 ppm in spectra of fresh samples (n=13), 1 day frozen samples (n=10) and 6 months frozen samples (n=9) of rat heart tissue. Relative integral was obtained by dividing the specific integral of the peak at 1.28 ppm by the overall integrated spectrum (from 0.6 ppm – 4.2 ppm) in each case.

After shock-freezing, the samples were kept in a freezer at – 80 °C (for at least 1 day to maximally 6 months) and measured again to observe the effect of the storing time on the MRS spectrum. No significant difference in lipid peaks was observed in the spectrum between 1 day frozen and 6 months frozen samples.

21 d acute EAM animals (male)

Animals with disease had a total weight of 232.50 g (±10.52 g) compared to 209.50 g (±6.41 g) for frozen controls. Heart weight was 1.34 g (±0.13 g) in myocarditis animals and 1.02 g (±0.04) in the correspondent controls. The ratio of heart weight to body weight (HW/BW) was significantly increased in myocarditis animals (21 d acute EAM: 5.80 g/kg (±0.70 g/kg), 21 d controls: 4.84 g/kg (±0.23 g/kg), $P<0.05$).

Histological and immunohistochemical analysis

The hearts of the rats were examined histologically (HE, Sirius red) and immunohistologically (CD68) on day 21 and investigated for cell infiltrations and fibrosis by the department of cardiovascular pathology at Deutsches Herzzentrum Berlin (Dr. Katharina Wassilew) (Figure 13). Fibrosis was assessed by calculating the collagen volume fraction (CVF) as the percentage of the pink-colored collagen from the total area in the Sirius red stained myocardial slices. No inflammatory infiltrate, low levels of collagen (< 5%) and no CD68 positive staining could be identified in control samples of healthy animals (group D). Histological analysis of 21 days myocarditis animals (group C) showed signs of highly flouride purulent inflammation with microabscess formation in the left ventricular and right ventricular myocardium in all samples. A mean of 38.7% (±9.6%) of the myocardial cross-section surface area of the short axis slice was infiltrated by inflammatory cells. Localization of the inflammatory infiltrate was mostly transmural, although the inner third of the myocardium closest to the endocardium was spared in 30% of the cases. CD68 staining indicating an infiltration with macrophages was strongly positive in 90% and discretely positive in 10% of the samples. Also, interstitial edema and pericarditis was confirmed in all samples. CVF was assessed in the Sirius red stained specimen revealing 12.4% (±3.3%) of fibrotic tissue.

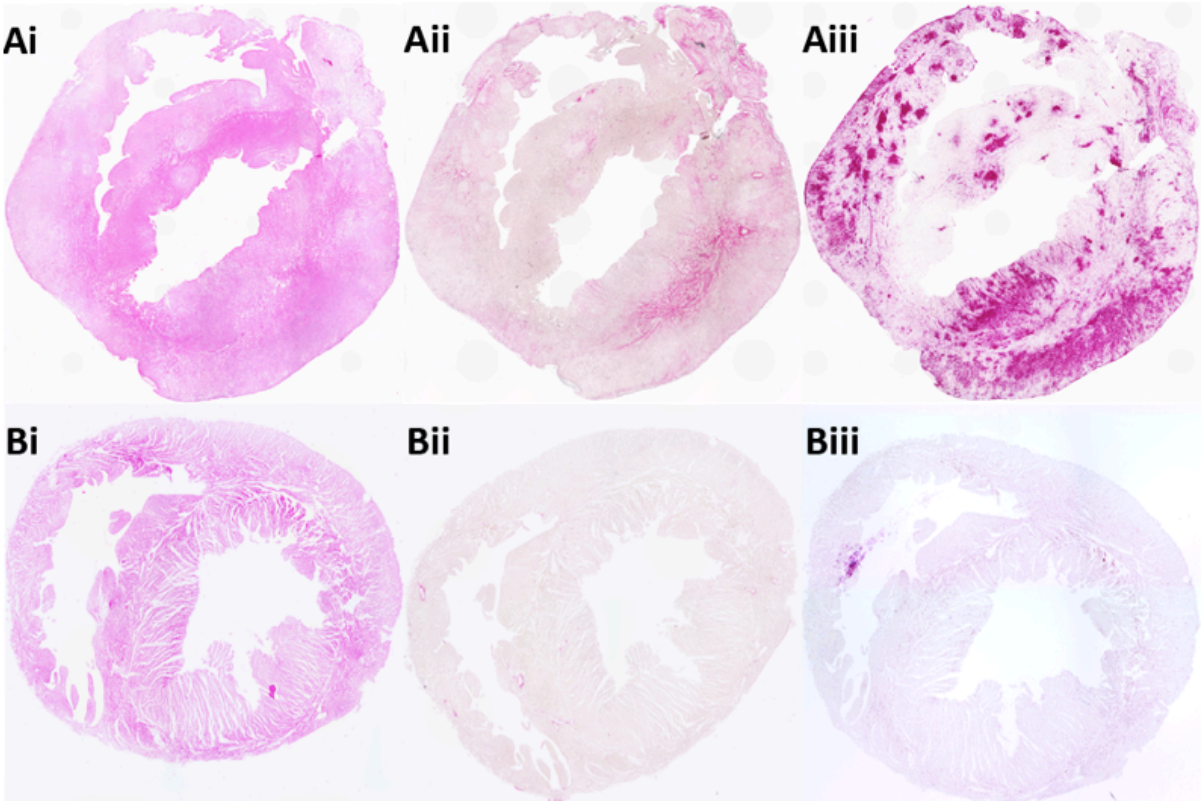

Figure 12: Histological findings of mid ventricular short axis slices of 21 d acute EAM (A) and 21 d acute controls (B) stained with HE (i), Sirius red (ii) and CD68 immunohistochemistry (iii)r. In Aiii, the myocardium is highly positive for CD68 staining, indicating the acute inflammation with inflammatory infiltrate. In Aii fibrosis calculated as the CVF affects especially the left ventricle.

The overall picture of the inflammation showed an active and ongoing process with typical signs of an **acute** inflammatory reaction.

Magnetic resonance spectroscopy (MRS)

For each animal, the proton spectrum was analyzed and investigated for differences between groups. Figure 14.A shows the spectral region of the creatine and taurine metabolites from one animal of each group. The ratio of Tau/Cr was calculated and compared between disease and control group. The ratio was 4.38 (±0.23) for 21 d acute EAM (4.13 (±0.32) for 21 d acute EAM-fresh) and 2.84 (±0.08) for 21 d control (2.59 (±0.09) for 21 d control-fresh) ($p<0.001$).

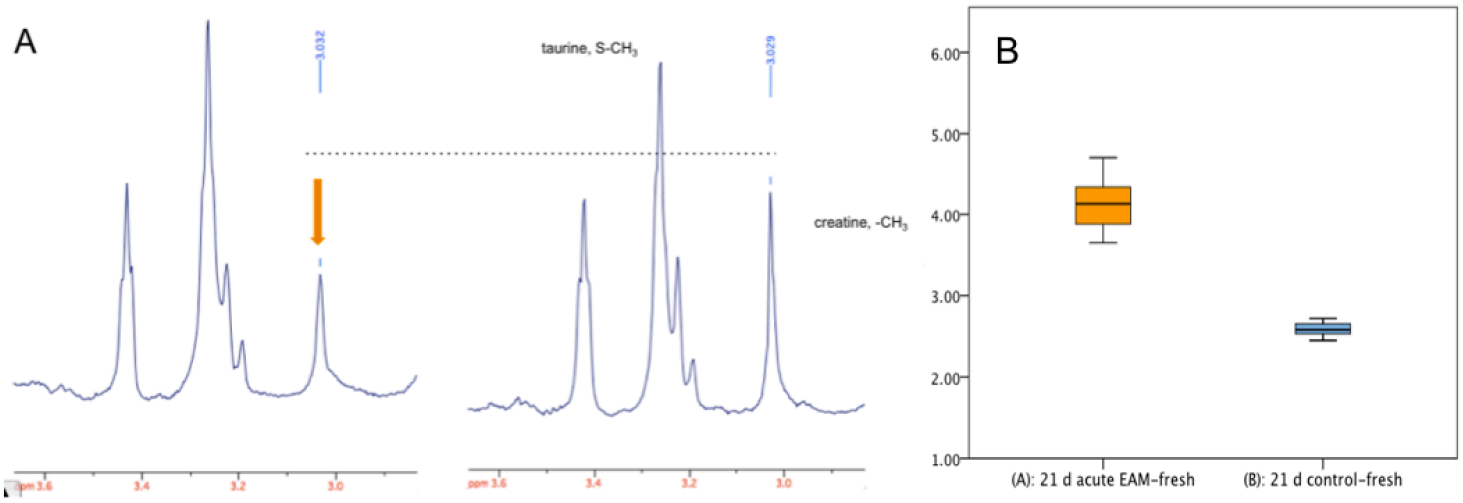

Figure 13: (A) Spectral region from 2.9 ppm to 3.6 ppm of one animal of 21 d acute EAM-fresh (left) and 21 d acute control-fresh (right). Spectra are normalized on taurine peak so that differences in the Tau/Cr ratio can be easily identified. Arrow indicates change in Tau/Cr ratio. (B) Tau/Cr ratio was found to be significantly different between 21 d acute EAM–fresh animals and 21 d control–fresh ($P<0.001$).

Evaluation of lipids in the 21 d acute EAM-fresh versus 21 d control-fresh using the methylene peak at 1.28 ppm demonstrated no significant change in lipid/taurine ratio (21 d acute EAM-fresh: 2.63 (±0.39), 21 d control-fresh: 2.50 (±0.30), $P>0.05$).

Correlation of MRS with other parameters

The Tau/Cr ratio was linearly correlated with the heart weight (HW) of 21 d acute EAM directly after explantation (Figure 15) and with the heart weight / body weight ratio (HW/BW) (Figure 16), respectively. Neither HW nor HW/BW correlated with the spectroscopy findings ($R<0.5$).

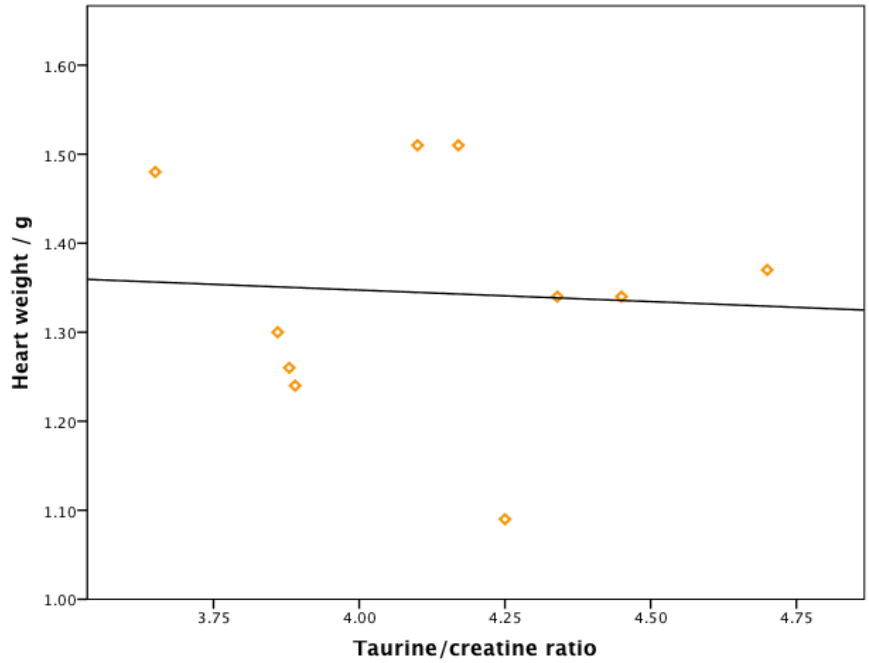

Figure 14: Scatter dot plot of correlation of heart weight versus Tau/Cr ratio with fitted regression line: no linear correlation could be observed (R<0.5).

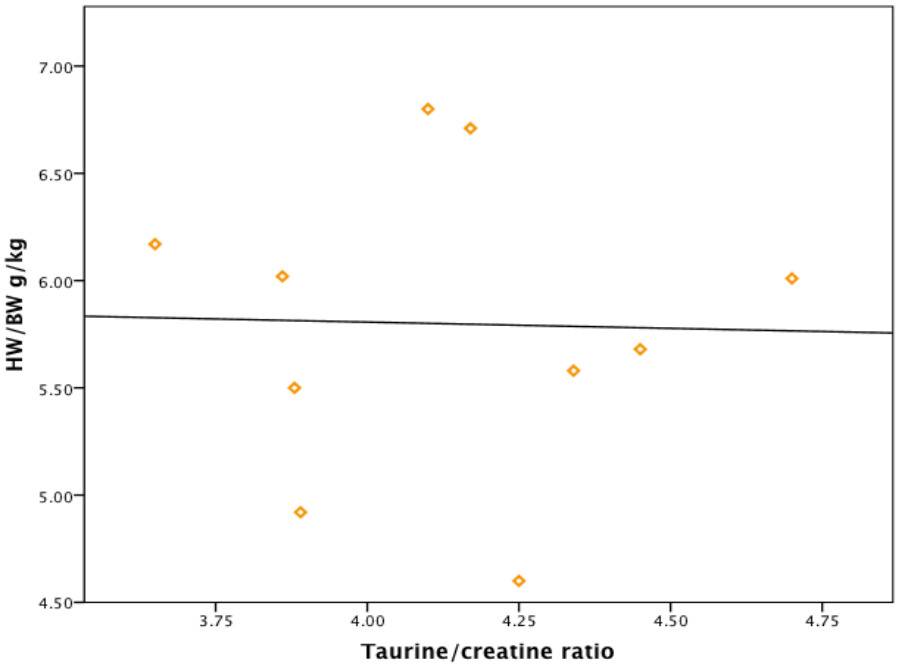

Figure 15: Scatter dot plot of correlation of HW/BW versus Tau/Cr ratio with fitted regression line: no linear correlation could be observed (R>0.5).

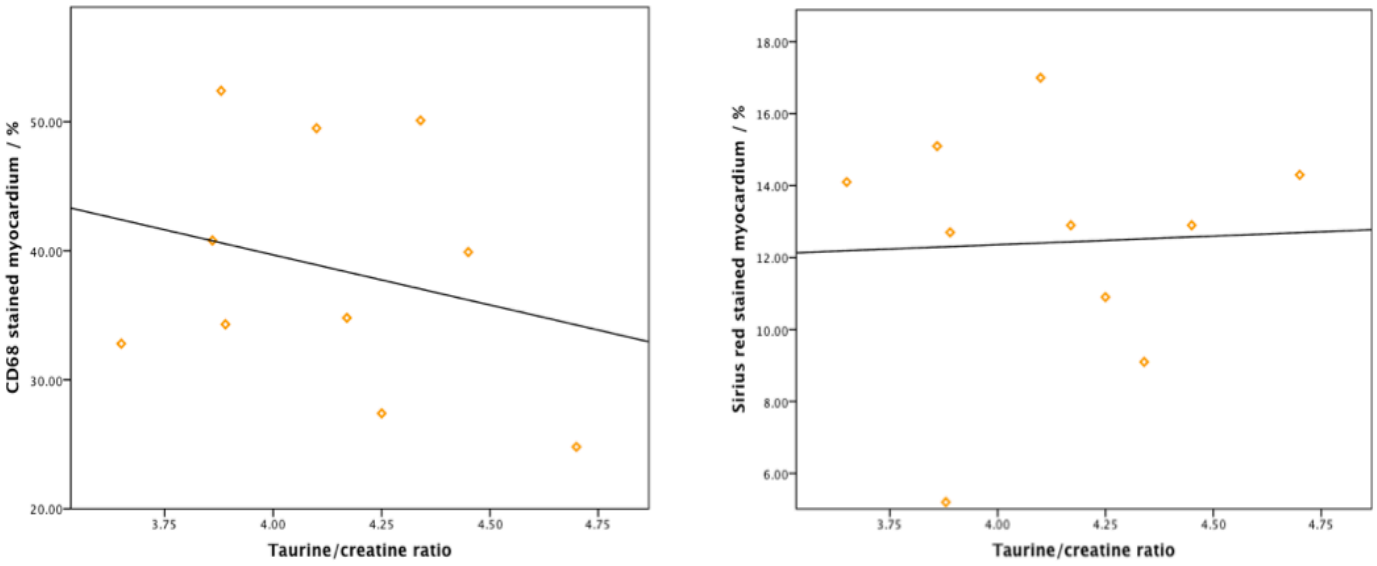

Figure 16: Scatter dot plot of correlation of percentage of CD68 stained myocardium (in mid ventricular slice of myocardium) versus Tau/Cr ratio (left) and of percentage of sirius red stained myocardium (in mid ventricular slice of myocardium) versus Tau/Cr ratio (right). No linear correlation could be observed (Pearson's correlation coefficient R<0.5).

Correlation analysis was also performed in MRS and histological/ immunohistochemical results of 21 d acute EAM animals (Figure 17). Tau/Cr ratio did not correlate linearly with percentage of CD68 stained myocardium and percentage of Sirius red stained myocardium, respectively. For both, Pearson's correlation coefficient was R<0.5.

35 d chronic EAM animals (male)

Animals with disease had a total weight of 300.0 g (±19.89 g) compared to 280.5 g (±37.63 g) for controls. Heart weight was 1.38 g (±0.14 g) in myocarditis animals and 1.01 g (±0.11) in the correspondent controls. The ratio of heart weight to body weight (HW/BW) was significantly increased in myocarditis animals (35 d chronic EAM: 4.65 g/kg (±0.67 g/kg), 35 d chronic control: 3.64 g/kg (±0.61 g/kg), P<0.01).

Histological and immunohistochemical analysis

The hearts of the rats were examined histologically (HE, Sirius red, CD68) on day 35 and investigated for cell infiltrations and fibrosis by the department of cardiovascular pathology at Deutsches Herzzentrum Berlin (Dr. Katharina Wassilew) (Figure 18). No inflammatory infiltrate, no collagen and no relevant CD68 positive staining could be identified in control samples of healthy animals. Histological analysis of 35 d chronic EAM animals showed signs of a slight inflammatory reaction in the myocardium without microabscess formation. A mean of 6.2% (±6.1%) of the myocardial cross-section surface area of the short axis slice was infiltrated by inflammatory cells. Localization of the inflammatory infiltrate was mostly located in the outer two thirds of the myocardium. CD68 staining indicating an infiltration with macrophages was positive in 80% and slightly positive in 20% of the samples.

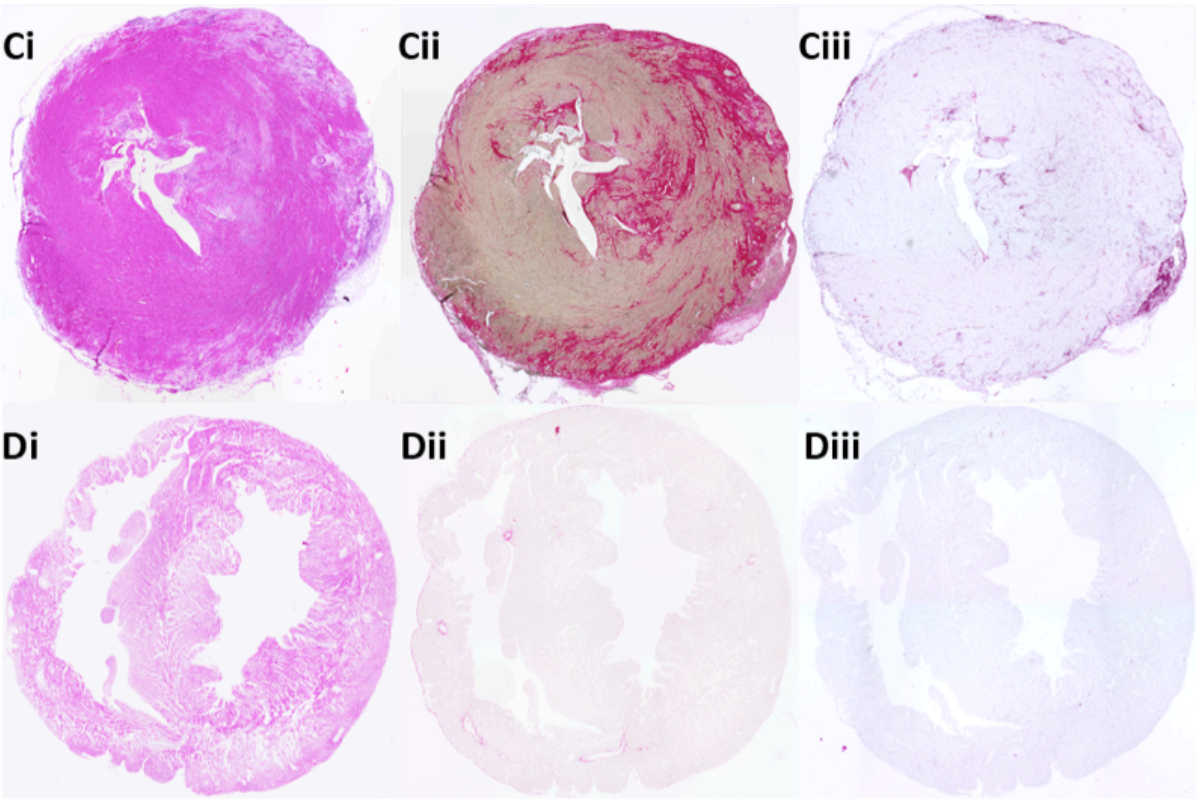

Figure 17: Histological findings of mid ventricular short axis slices of 35 d chronic EAM (C) and 35 d control (D) stained with HE (i), Sirius red (ii) and CD68 immunohistochemistry (iii): In Cii, the myocardium shows a high degree of fibrosis calculated as the CVF, which is typical for the chronic phase in EAM (with low inflammatory cell infiltrate in Ciii).

Interstitial edema was confirmed in 50% of the samples. The CVF was assessed in the Sirius red stained samples and led to a value of 21.8% (±11.5%) of the myocardial cross-section surface area of the short axis slice as fibrotic tissue. The overall picture corresponded to a typical **chronic** inflammatory reaction.

Cardiac magnetic resonance (CMR)

Three myocarditis animals died during CMR acquisition before relevant data could be obtained, but heart samples were collected and shock frozen immediately after death for MRS analysis.

LVEF was reduced in the animals with chronic myocarditis (compared to controls (55.2% ±11.3% vs. 72.6% ±3.8%, $P<0.01$) as determined by multi-slice short axis analysis throughout the whole heart. Left ventricular end-diastolic volume (LVEDV) was also increased (0.47 ml ±0.11 ml versus 0.35 ml ±0.05 ml, $P<0.05$). Figure 19 illustrates the increased left-ventricular volume and reduced systolic contraction in a chronic myocarditis animal as compared to a control animal on end-diastolic and end-systolic short axis cine images.

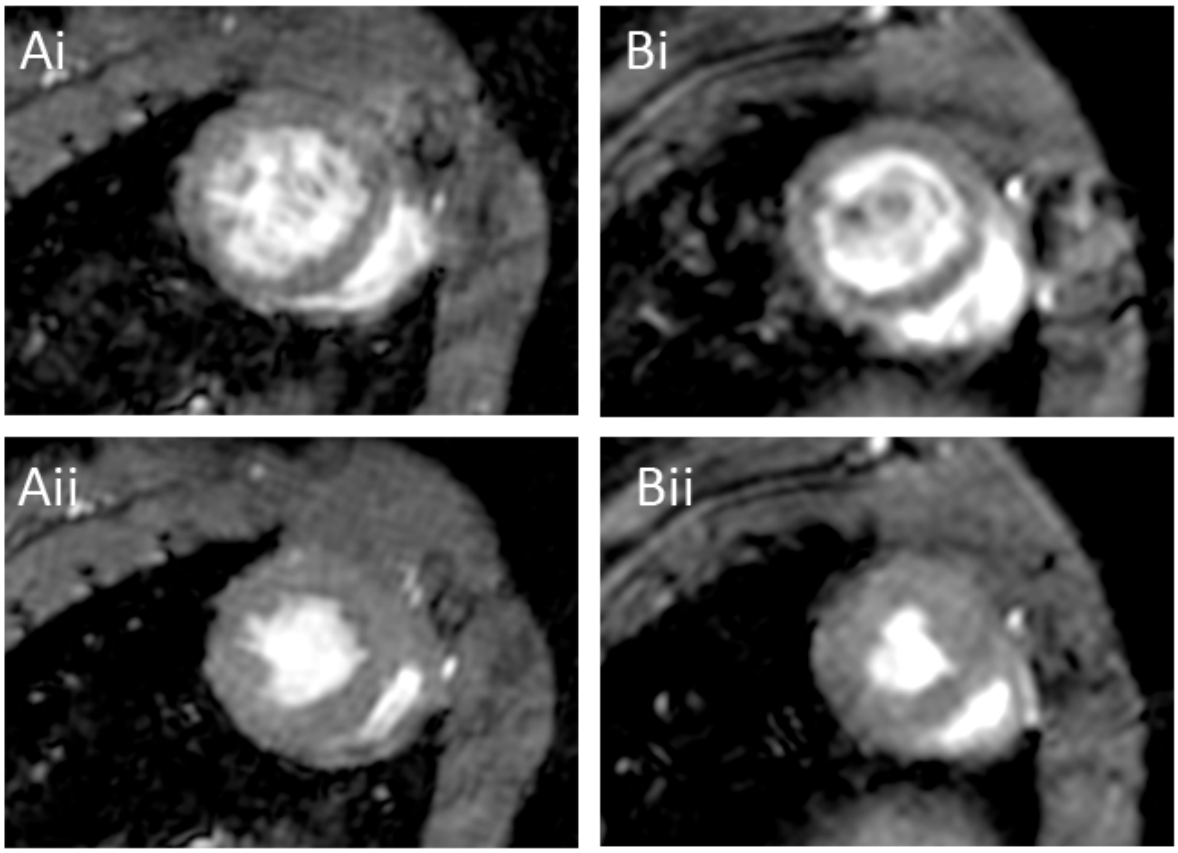

Figure 18: Short axis images of an animal from the 35 d chronic EAM group (Ai in end-diastole, Aii end-systole) and a 35 d control animal (Bi in end-diastole, Bii in end-systole). Large hearts (confirmed by the HW/BW values between groups) and reduced systolic contraction indicate secondary DCM in the diseased heart.

Magnetic resonance spectroscopy (MRS)

For each animal, the proton spectrum was analyzed and investigated for differences between groups. Figure 20.A shows the spectral region of the creatine and taurine metabolites, which are two of the most abundant small molecules in the heart. The ratio of Tau/Cr was calculated and compared between disease and control group. The ratio was 4.47 (±0.83) for 35 d chronic EAM animals and 2.59 (±0.38) for 35 d chronic controls. The change in this particular ratio was found to be highly significant between diseased and control groups ($P<0.001$).

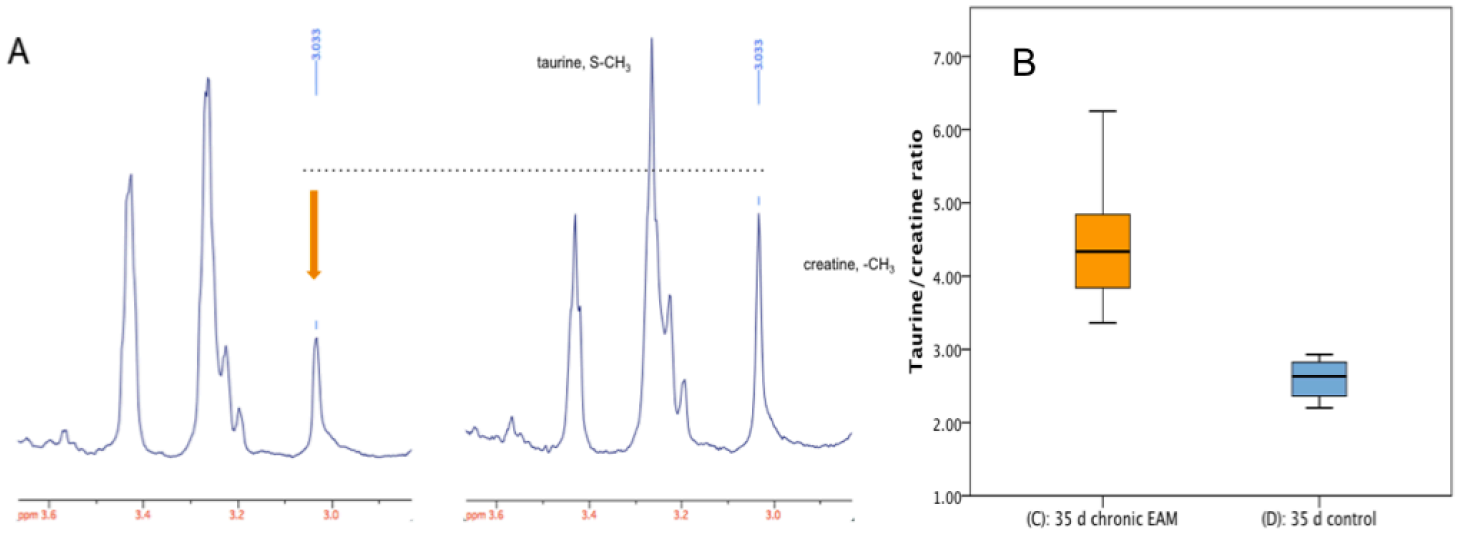

Figure 19: (A) Spectral region from 2.9 ppm to 3.6 ppm of one animal from the 35 d chronic EAM group (left) vs. one from the 35 d control group (right). Spectra are normalized on taurine peak so that differences in the Tau/Cr ratio can be easily seen. Arrow indicates change in Tau/Cr ratio. (B) Tau/Cr ratio was found to be significantly different between disease group and control ($P<0.001$).

Lipids could not be evaluated in the 35 d chronic EAM group versus frozen controls due to the aforementioned changes in lipid peaks after shock freezing in liquid nitrogen.

Correlation of MRS with other parameters

There was a strong negative correlation of LVEF with Tau/Cr ratio with a Pearson's correlation coefficient of $R=0.937$ ($P<0.001$) (Figure 21). All healthy animals had a high ejection fraction and a low Tau/Cr ratio. Animals with myocarditis but preserved ejection fraction had relatively low Tau/Cr ratios as well, whereas animals whose function was strongly impaired (low LVEF) had high Tau/Cr ratios.

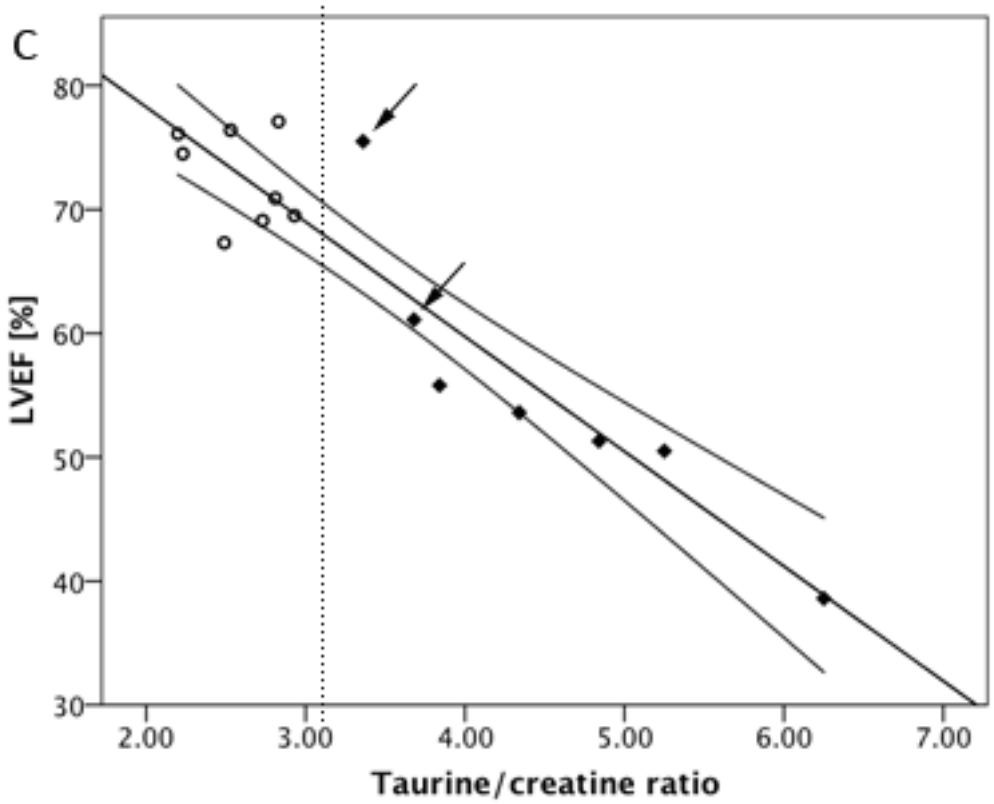

Figure 20: Linear correlation of Tau/Cr ratio versus LVEF with fitted regression line and 95% confidence intervals. Full rhombuses correspond to 35 d chronic EAM animals and empty circles correspond to healthy 35 d control animals. Pearson's correlation coefficient was R=0.937 (P<0.001). The cut-off value of 3.10 in the Tau/Cr ratio is indicated as dotted line. Arrows indicate animals that had normal functional parameters (LVEF > 60) but showed increased Tau/Cr ratio.

There was a moderate negative correlation of LVEDV with the Tau/Cr with a Pearson's coefficient of R=0.790 (P<0.01). The correlation appeared similar to the results found with LVEF: all healthy animals had low end-diastolic volumes and low Tau/Cr ratios, whereas in the myocarditis animals, the higher the Tau/Cr ratio, the higher was the LVEDV. A cut-off value of 3.10 in the Tau/Cr ratio was able to distinguish between hearts with and without myocarditis with both sensitivity and specificity of 100%, even in cases where LVEF and LVEDV, respectively were found to be normal (Figure 21 and 22).

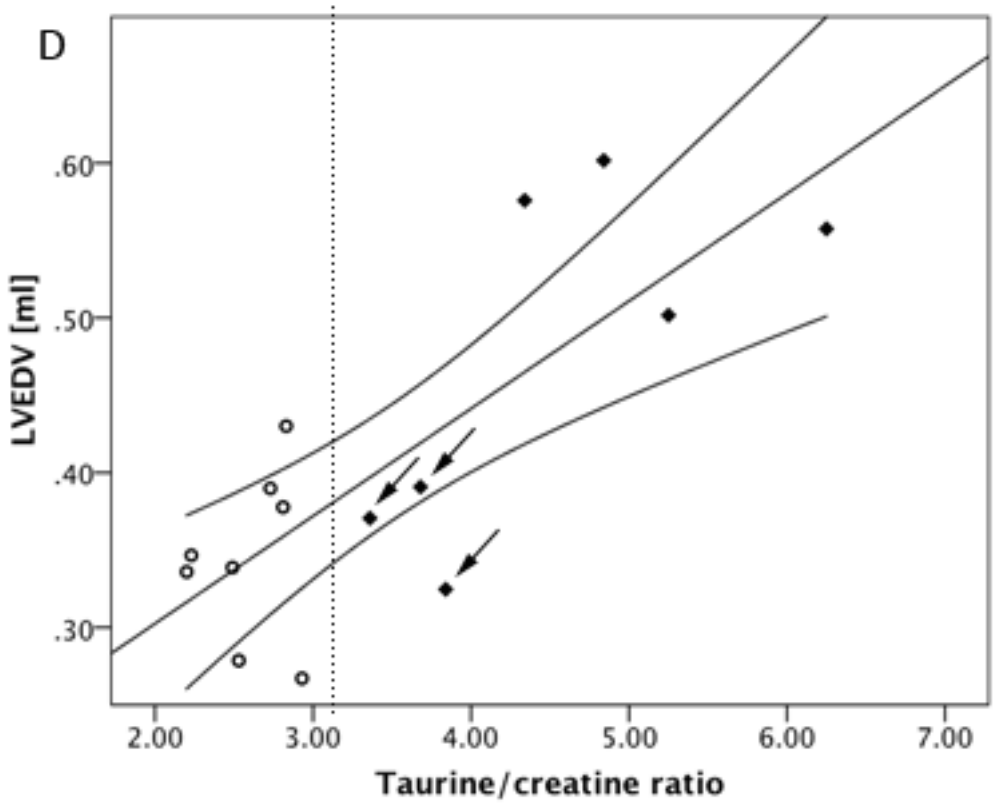

Figure 21: Linear correlation of Tau/Cr ratio versus LVEDV with fitted regression line and 95% confidence intervals. Full rhombuses correspond to 35 d chronic EAM animals and empty circles correspond to healthy 35 d control animals. Pearson's correlation coefficient was R=0.790 (P<0.01). The cut-off value of 3.10 in the Tau/Cr ratio is indicated as dotted line. Arrows indicate animals that have normal functional parameters (LVEDV < 45 ml) but show increased Tau/Cr ratio.

The Tau/Cr ratio was linearly correlated with the heart weight (HW) of 35 d chronic animals directly after explantation (Figure 23) and with the heart weight / body weight ratio (HW/BW) (Figure 24), respectively. HW/BW correlated to a higher extent with the spectroscopy resulting in a Pearson correlation coefficient of R=0.749 (P<0.05), whereas HW values alone correlated with a coefficient of R=0.617 (P>0.05). HW/BW may give a better estimation of how strong the heart disease of a single animal is evolved, based on the fact that bigger animals intrinsically have bigger hearts as well.

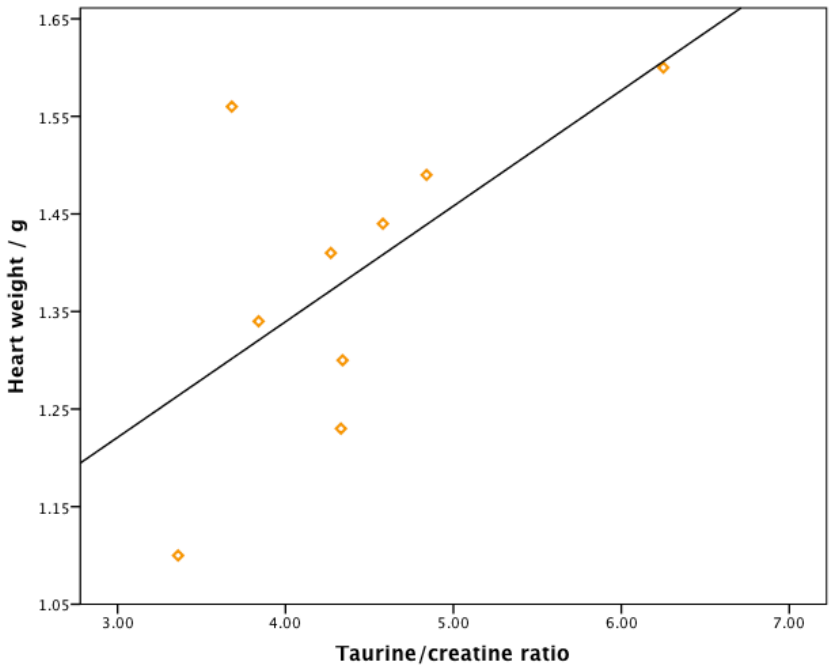

Figure 22: Linear correlation of heart weight vs. Tau/Cr ratio of 35 d chronic EAM animals with fitted regression line. Pearson's correlation coefficient was R=0.617 (P>0.05).

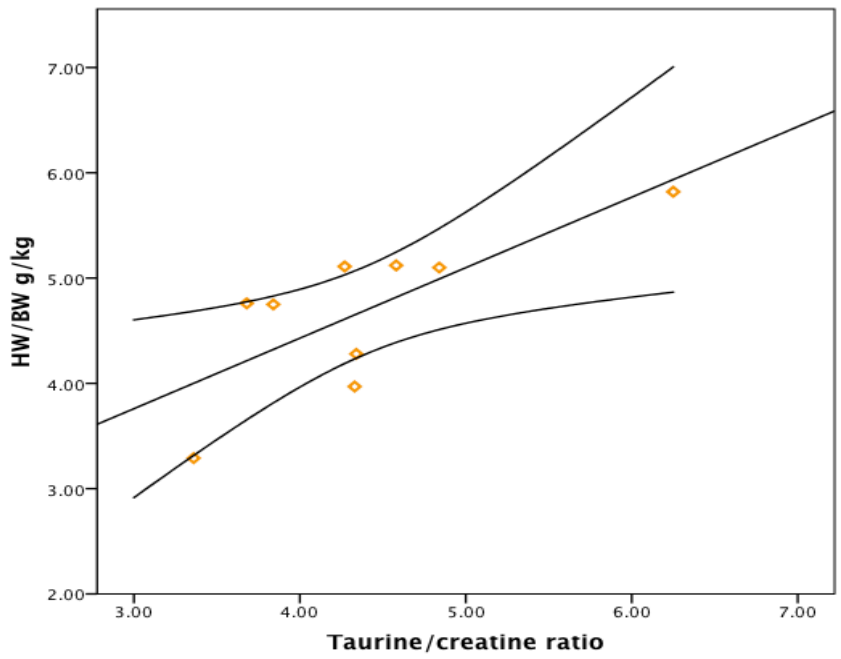

Figure 23: Linear correlation of HW/BW versus Tau/Cr ratio 35 d chronic EAM animals with fitted regression line and 95% confidence intervals. Pearson's correlation coefficient was R=0.749 (P<0.05)

MRS results were also compared to histological and immunohistochemical results of myocarditis animals (Figure 25). Tau/Cr ratio did not correlate linearly with

percentage of CD68 stained myocardium and percentage of Sirius red stained myocardium, respectively. For both, Pearson's correlation coefficient was R<0.5.

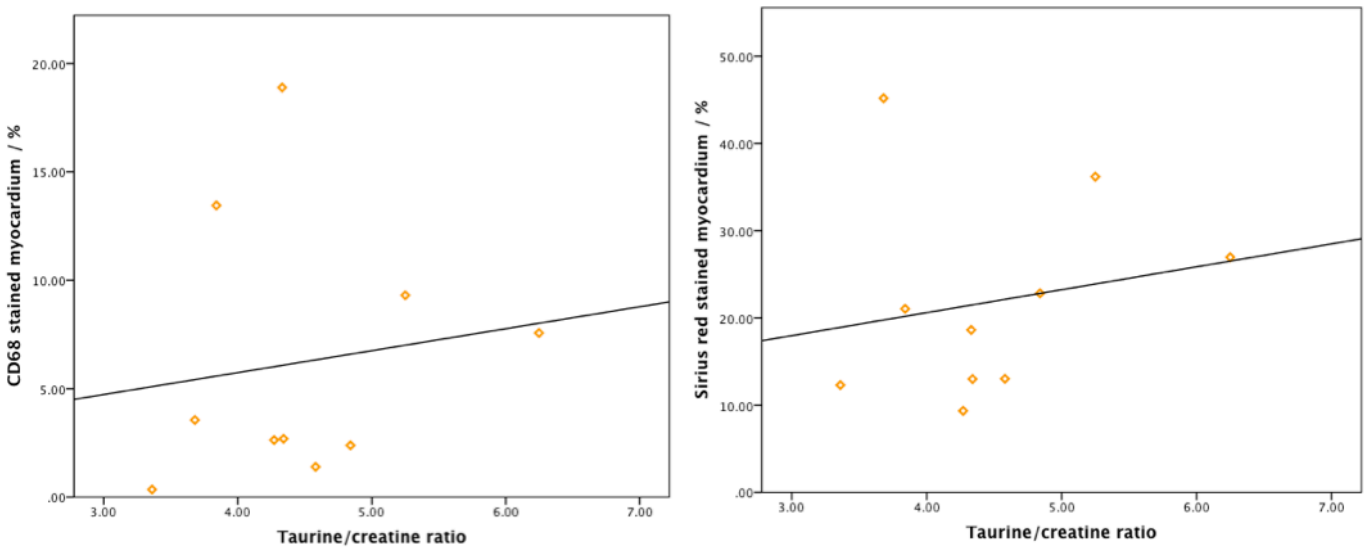

Figure 24: Scatter dot plot of correlation of percentage of CD68 stained myocardium (in mid ventricular slice of myocardium) versus Tau/Cr ratio (left) and of percentage of sirius red stained myocardium (in mid ventricular slice of myocardium) versus Tau/Cr ratio (right) of 35 d chronic EAM animals. No linear correlation could be observed (Pearson's correlation coefficient R<0.5).

Direct comparison: 21 d acute EAM vs 35 d chronic EAM and controls

Comparison of the groups A, B, C and D in Figure 25 to visualize the fact that the differences between groups are similar in the acute as well as in the chronic myocarditis animals.

Magnetic resonance spectroscopy (MRS).

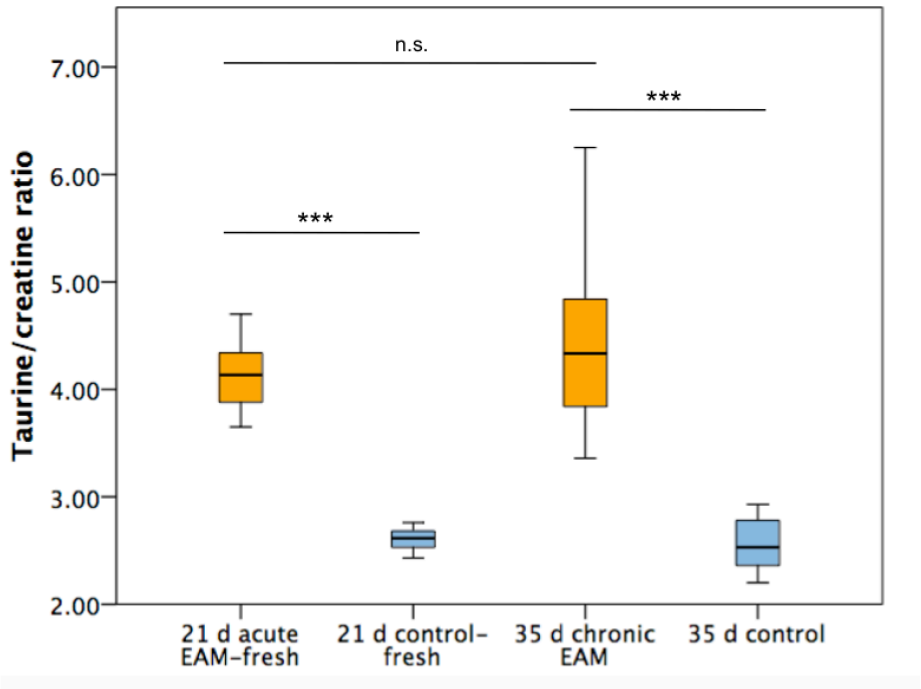

Figure 27: Overview of both male disease groups (21 d acute EAM and 35 d chronic EAM). As previously stated Tau/Cr ratio was found to be significantly different between disease groups and controls (P<0.001). As for comparison of acute and chronic animals, no statistically significant difference was found.

Discussion

Our study demonstrates that the metabolic ratio of myocardial Tau/Cr as detected by proton MRS is able to differentiate between healthy myocardium and myocardium with EAM in rats. Tau/Cr ratio not only correlates with functional parameters as detected in CMR (LVEF, LVEDV), but also detects diseased animals with normal functional parameters.

The diagnosis and monitoring of myocarditis can be considered on different levels. On an organ level, methods such as 2D echocardiography or cine MRI allow the detection of changes in cardiac function and ventricular remodelling. On a tissue level, MRI has been shown to detect myocardial edema (using T2-weighted techniques [27] or parametric mapping [34]) and focal inflammatory lesions (using late gadolinium enhancement [100]). On the cellular level, *molecular imaging* of disease-specific molecular targets using nuclear medicine and MRI offers approaches focused on marking inflammatory cells [101] [102]. Due to a variety of reasons, including limited sensitivity and significant toxicity of molecular probes, none of these cell-level techniques have found their way into clinical routine.

A number of studies have demonstrated the feasibility and diagnostic potential of ^{31}P-MRS for the assessment of cardiac metabolism [103] [104] [105]. This approach enables the quantification of ATP, ADP and phosphocreatine, but it is technically demanding not only because of the need for multi-nuclei-enabled MR systems and specific coils, but also due to the low proportion of phosphorus in the body when compared to hydrogen protons and thus low signal-to-noise ratio and long scan times. The recent introduction of dynamic hyperpolarization (DNP) [106] provides the potential to visualize the metabolism of hyperpolarized carbon-based probes such as pyruvate. However, this approach not only requires multi-nuclei-enabled MR systems and specific coils, but also an on-site DNP polarizer for the production of hyperpolarized ^{13}C agents. In contrast, proton MRS utilizes the same nucleus as standard MRI, aiming to analyze the spectrum and distribution of compounds that together generate the standard imaging signal. There is no need for specific

hardware, and the resulting signal is relatively high compared to other non-hyperpolarized spectroscopic MR approaches. Proton-containing molecules of interest for cardiac metabolism include creatine, phosphocreatine and lipids.

We demonstrated significant differences in the ratio of myocardial Tau/Cr between healthy myocardium and myocardium from rats with EAM as detected by proton MRS. Similar alterations in the creatine to taurine ratio have been found in the urinary MRS profile of patients with ischemic heart failure [107]. The change of Tau/Cr ratio in 21 d acute EAM indicates that metabolic alterations occur acutely with the development of myocarditis.

Taurine increase has been described in inflammatory processes, which may explain the higher Tau/Cr as a result of myocardial inflammation [88] [108]. The change of the ratio during the acute phase with a lot of inflammatory cellular infiltrate would seem to support this theory. On the other hand, HF models in animals and in-vivo measurements in humans showed that metabolic alterations, including depletion of creatine occurred in HF [54] [55] [98]. A depletion in creatine would also be consistent with our results of a higher Tau/Cr ratio in EAM. There are several other reasons to believe that a depletion in creatine might be the main driver of the observed changes in Tau/Cr in our study. First, the Tau/Cr ratio changed equally for both the acute myocarditis group (21 d acute EAM) and the chronic myocarditis group (35 d chronic EAM), whereas the corresponding histological analysis could distinguish between acute myocarditis with highly inflammatory tissue and a more chronic myocarditis with a mild inflammatory reaction. Second, there was a positive correlation of LVEF with the Tau/Cr ratio change in chronic myocarditis. But the most probable explanation seems to be that both mechanisms are present in myocarditis (taurine increase AND creatine depletion).

One very important finding in our analysis is that an abnormal Tau/Cr ratio was able to detect myocarditis in animals even when the LVEF or LVEDV was within the normal range (2 animals with normal LVEF, 3 animals with normal LVEDV). This is a highly interesting, as it shows that although Tau/Cr and LVEF results correlate (and do so better the higher the Tau/Cr ratio and the lower the LVEF), MRS was able to detect individual animals that had the disease but showed no functional impairment. As functional impairment is correlated with creatine depletion in the literature sources [54] [55], this finding may then again lead us to the conclusion that taurine increase

in inflammation is significantly involved in the alteration in the Tau/Cr ratio. In this particular experiment, Tau/Cr ratio was thus better suited to detect and diagnose animals with the disease than LVEF as obtained from MRI. If in-vivo experiments would lead to equivalent results, some myocarditis cases, which may so far have been missed based on functional assessment, might be detected and monitored accordingly. This demonstrates the potential of this method in assisting in the diagnosis of myocarditis and inflammatory cardiomyopathy. MRS may possibly be considered as an additional diagnostic tool. Sensitivity and specificity of this method to identify diseased animals were very high (100% and 100%, respectively). On the other hand, MRS might not be able to differentiate between myocarditis and other diseases that might exhibit altered cardiac metabolism as well (e.g. other forms of heart failure).

The Tau/Cr ratio is not affected by the shock-freezing procedure either, fresh and frozen disease and control groups, had similar values. We found that once shock frozen in liquid nitrogen, the samples were stable for months when stored at -80 °C. This facilitated the planning of further ex-vivo experiments, and allowed for batch processing of the samples, rather than processing them individually after the harvesting of each heart. To allow comparison of the MRI results with ex-vivo MRS results, it is important to know that freezing does not change this particular region of the spectrum, as high-resolution MRS facilities are usually located at chemical research departments which might not have animal housing facilities. Animals that are in the acute phase of the disease are extremely sensitive and would most probably not survive transportation between facilities, so that examination of fresh samples would not be possible.

The lipid / taurine ratio was used in our study to compare a possible lipid content variation between healthy and diseased animals, but no significant difference was found. The evaluation of this ratio was only possible in the fresh groups (21 d acute EAM-fresh, 21 d control-fresh) due to changes of lipid peaks after freezing. Assuming a relatively constant level of taurine (as with the Tau/Cr ratio), we could conclude that lipids do not accumulate in the myocardium in the acute phase of myocarditis. In the literature, intramyocardial lipid accumulation has been discussed in the context of metabolism of the failing heart. Studies e.g. by Nakae et al. [98]

showed that there is no correlation between lipid concentration and LVEF in DCM and that lipid concentration correlated with BMI. This would be consistent with our results, although we only studied acute phase myocarditis, which in a later phase may lead to DCM. In general, the lipid content has been found to depend primarily on the feeding state, level of exercise, and metabolic diseases like diabetes and obesity [109]. In myocardial infarction, changes in lipid content have been detected by magnetic resonance spectroscopy [110], indicating that myocardial lipid deposition started already 6h after coronary artery occlusion.

The assessment of metabolic changes in the myocardium and in muscle tissue in general differs from other tissue in the way that muscular diseases lead to quantitative rather than qualitative changes in metabolites. Tumors are well known to produce specific metabolites, which makes them an easier target for specific spectroscopic measurements [117] [118] [80] [81]. Also, tissue from mucosae, liver and kidneys possess a large variety of different metabolic pathways with small molecule metabolites, which can be detected by spectroscopy and might be altered in diseased states of the organ [79] [119]. When cardiac metabolism is affected, there are proportional changes within the set of given metabolites rather than shifts towards new metabolites, which makes detection and interpretation easier but rather non-specific [73] [60].

Clinical impact. The integration of in-vivo metabolic imaging into conventional MRI protocols would add a new layer of information to clinical cardiac imaging. There are several pulse sequences available (e.g. PRESS, STEAM) that allow for in-vivo ^{1}H-MR single-voxel spectroscopy or multi-voxel spectroscopic imaging [120] [121]. 3T MR systems are now widely available and are able to provide high-quality MRS data within <10 minutes. Thus, the integration of ^{1}H-MRS for the assessment of cardiac metabolism into clinical routine protocols seems feasible but requires further development of standardized post-processing and analysis tools.

Limitations. High resolution MAS (HR-MAS) is mentioned in the literature as a means of achieving an additional increase of spectral resolution compared to

standard MAS [122] [123] [124]. This method requires an additional transmission channel on the MR spectrometer to emit radio waves on the deuterium frequency of D_2O to stabilize the experiment in case of shifting of the magnetic field. This hardware was not available for our study, but resolution was found to be very good nevertheless, as illustrated in Figure 8. Multiplets such as the taurine triplets (taurine (S-CH_3), 3.26 ppm, t; taurine (N-CH_3), 3.48 ppm, t), the lactate doublet (lactate (-CH_3), 1.33 ppm, d) and the alanine doublet (alanine (-CH_3), 1.47 ppm, d) were well resolved in all fresh spectra. Also, various relatively close peaks in the spectral region between 2.0 ppm and 2.5 ppm (lipids, 2.04 ppm; glutamine (β-CH_3), 2.14 ppm; lipids, 2.24 ppm; glutamate (γ-CH_3), 2.35 ppm; glutamine (γ-CH_3), 2.45 ppm) could be easily differentiated. The high resolution was reproducible in all samples and was slightly lower in the spectra of frozen samples.

TSP used as external standard in water [125] was found to have low reproducibility in our MAS-MRS experiments. Thus, no external standard was used and absolute quantification of lipids, taurine and creatine was not possible. Our MRS results are of a relative nature, although evidence indicates that the ratio change is based on a creatine decrease rather than taurine increase. Another method that could be applied for quantitative measurements is electronic reference to in-vivo concentrations (ERETIC) [125]. This is a pulse technique that employs a synthesized RF pulse during the acquisition period to produce its signal from which quantitative information about metabolites can be derived. As no chemical substance is added, there are no concerns about toxicity to the tissue, chemical activity, binding and volatility. Furthermore ERETIC has been shown to provide reproducible and stable quantitative results with HR-MAS MR spectroscopy. Unfortunately, this method requires multi-channel capabilities and specific pulse sequences that were not available in our experimental setting. Other analytic methods such as high-pressure liquid chromatography could also be used for quantitative analysis concomitantly with the MRS measurements. Also, the water peak is often used as an internal standard in in-vivo experiments [98]. However, interstitial edema, which was confirmed histologically in the myocarditis animals, may intrinsically change the water content of a sample and interfere with this technique.

The number of animals in each group was relatively small, especially in the control groups (7 and 8 animals). This must be considered when interpretating the results. The same applies to the correlation of LVEF and LVEDV with Tau/Cr ratio, as only 7 myocarditis animals survived the MRI scanning.
Finally, we did not test the performance of MRS in other models of HF than EAM. Thus, our data do not allow us to comment on the specificity of MRS for differentiating EAM from other myocardial diseases.

Conclusions. Our study shows that metabolic alterations occur acutely with the development of myocarditis and that myocardial Tau/Cr ratio as detected by proton MRS is able to differentiate between healthy and diseased myocardium in rats with acute and chronic EAM. Tau/Cr ratio correlates strongly with LVEF when both parameters show pathologic values, and furthermore, it detects diseased animals even when function is considered normal. ^{1}H-MRS reveals metabolic information in the course of inflammatory heart disease and might be of additional diagnostic value in the non-invasive assessment of myocarditis.

References

1. **Report of the 1995 World Health Organization/International Society and Federation of Cardiology Task Force on the Definition and Classification of Cardiomyopathies**. *Circulation* 1996, **93**:841–842.

2. Elliott P, Andersson B, Arbustini E, Bilinska Z, Cecchi F, Charron P, Dubourg O, Kühl U, Maisch B, McKenna WJ, Monserrat L, Pankuweit S, Rapezzi C, Seferovic P, Tavazzi L, Keren A: **Classification of the cardiomyopathies: a position statement from the European Society Of Cardiology Working Group on Myocardial and Pericardial Diseases.** *Eur Heart J* 2008, **29**:270–6.

3. Schultz JC, Hilliard AA, Cooper LT, Rihal CS: **Diagnosis and treatment of viral myocarditis.** *Mayo Clin Proc* 2009, **84**:1001–9.

4. Breinholt JP, Moulik M, Dreyer WJ, Denfield SW, Kim JJ, Jefferies JL, Rossano JW, Gates CM, Clunie SK, Bowles KR, Kearney DL, Bowles NE, Towbin JA: **Viral epidemiologic shift in inflammatory heart disease: the increasing involvement of parvovirus B19 in the myocardium of pediatric cardiac transplant patients.** *J Heart Lung Transplant* 2010, **29**:739–46.

5. Hidron A, Vogenthaler N, Santos-Preciado JI, Rodriguez-Morales AJ, Franco-Paredes C, Rassi A: **Cardiac involvement with parasitic infections.** *Clin Microbiol Rev* 2010, **23**:324–49.

6. Kilian JG, Kerr K, Lawrence C, Celermajer DS: **Myocarditis and cardiomyopathy associated with clozapine**. *Lancet* 1999, **354**:1841–1845.

7. Stelts S, Taylor MH, Nappi J, Van Bakel AB: **Mesalamine-associated hypersensitivity myocarditis in ulcerative colitis.** *Ann Pharmacother* 2008, **42**:904–5.

8. Nunes H, Freynet O, Naggara N, Soussan M, Weinman P, Diebold B, Brillet P-Y, Valeyre D: **Cardiac sarcoidosis.** *Semin Respir Crit Care Med* 2010, **31**:428–41.

9. Cooper LT: **Giant cell and granulomatous myocarditis.** *Heart Fail Clin* 2005, **1**:431–7.

10. Rose NR: **Myocarditis: infection versus autoimmunity.** *J Clin Immunol* 2009, **29**:730–7.

11. Caforio ALP, Pankuweit S, Arbustini E, Basso C, Gimeno-Blanes J, Felix SB, Fu M, Heliö T, Heymans S, Jahns R, Klingel K, Linhart A, Maisch B, McKenna W, Mogensen J, Pinto YM, Ristic A, Schultheiss H-P, Seggewiss H, Tavazzi L, Thiene G, Yilmaz A, Charron P, Elliott PM: **Current state of knowledge on aetiology, diagnosis, management, and therapy of myocarditis: a position statement of the European Society of Cardiology Working Group on Myocardial and Pericardial Diseases.** *Eur Heart J* 2013, **34**:2636–48, 2648a–2648d.

12. Kindermann I, Barth C, Mahfoud F, Ukena C, Lenski M, Yilmaz A, Klingel K, Kandolf R, Sechtem U, Cooper LT, Böhm M: **Update on myocarditis.** *J Am Coll Cardiol* 2012, **59**:779–92.

13. Towbin JA, Lowe AM, Colan SD, Sleeper LA, Orav EJ, Clunie S, Messere J, Cox GF, Lurie PR, Hsu D, Canter C, Wilkinson JD, Lipshultz SE: **Incidence, causes,**

and outcomes of dilated cardiomyopathy in children. *JAMA* 2006, **296**:1867–76.

14. D'Ambrosio A: **The fate of acute myocarditis between spontaneous improvement and evolution to dilated cardiomyopathy: a review**. *Heart* 2001, **85**:499–504.

15. GORE I, SAPHIR O: **Myocarditis; a classification of 1402 cases.** *Am Heart J* 1947, **34**:827–30.

16. Basso C: **Postmortem diagnosis in sudden cardiac death victims: macroscopic, microscopic and molecular findings**. *Cardiovasc Res* 2001, **50**:290–300.

17. Fabre A, Sheppard MN: **Sudden adult death syndrome and other non-ischaemic causes of sudden cardiac death.** *Heart* 2006, **92**:316–20.

18. Heymans S: **Myocarditis and heart failure: need for better diagnostic, predictive, and therapeutic tools.** *Eur Heart J* 2007, **28**:1279–80.

19. Sagar S, Liu PP, Cooper LT: **Myocarditis.** *Lancet* 2012, **379**:738–47.

20. Kawai C: **From myocarditis to cardiomyopathy: mechanisms of inflammation and cell death: learning from the past for the future.** *Circulation* 1999, **99**:1091–100.

21. Liu PP, Mason JW: **Advances in the Understanding of Myocarditis**. *Circulation* 2001, **104**:1076–1082.

22. Caforio ALP, Mahon NG, Baig MK, Tona F, Murphy RT, Elliott PM, McKenna WJ: **Prospective familial assessment in dilated cardiomyopathy: cardiac autoantibodies predict disease development in asymptomatic relatives.** *Circulation* 2007, **115**:76–83.

23. Caforio ALP, Pankuweit S, Arbustini E, Basso C, Gimeno-Blanes J, Felix SB, Fu M, Heliö T, Heymans S, Jahns R, Klingel K, Linhart A, Maisch B, McKenna W, Mogensen J, Pinto YM, Ristic A, Schultheiss H-P, Seggewiss H, Tavazzi L, Thiene G, Yilmaz A, Charron P, Elliott PM: **Current state of knowledge on aetiology, diagnosis, management, and therapy of myocarditis: a position statement of the European Society of Cardiology Working Group on Myocardial and Pericardial Diseases.** *Eur Heart J* 2013, **34**:2636–48, 2648a–2648d.

24. Leone O, Veinot JP, Angelini A, Baandrup UT, Basso C, Berry G, Bruneval P, Burke M, Butany J, Calabrese F, d'Amati G, Edwards WD, Fallon JT, Fishbein MC, Gallagher PJ, Halushka MK, McManus B, Pucci A, Rodriguez ER, Saffitz JE, Sheppard MN, Steenbergen C, Stone JR, Tan C, Thiene G, van der Wal AC, Winters GL: **2011 consensus statement on endomyocardial biopsy from the Association for European Cardiovascular Pathology and the Society for Cardiovascular Pathology.** *Cardiovasc Pathol* , **21**:245–74.

25. Cooper LT, Baughman KL, Feldman AM, Frustaci A, Jessup M, Kuhl U, Levine GN, Narula J, Starling RC, Towbin J, Virmani R: **The role of endomyocardial biopsy in the management of cardiovascular disease: a scientific statement from the American Heart Association, the American College of Cardiology, and the European Society of Cardiology. Endorsed by the Heart Failure Society of**. *J Am Coll Cardiol* 2007, **50**:1914–31.

26. Baccouche H, Mahrholdt H, Meinhardt G, Merher R, Voehringer M, Hill S, Klingel K, Kandolf R, Sechtem U, Yilmaz A: **Diagnostic synergy of non-invasive**

cardiovascular magnetic resonance and invasive endomyocardial biopsy in troponin-positive patients without coronary artery disease. *Eur Heart J* 2009, **30**:2869–79.

27. Abdel-Aty H, Boyé P, Zagrosek A, Wassmuth R, Kumar A, Messroghli D, Bock P, Dietz R, Friedrich MG, Schulz-Menger J: **Diagnostic performance of cardiovascular magnetic resonance in patients with suspected acute myocarditis: comparison of different approaches.** *J Am Coll Cardiol* 2005, **45**:1815–22.

28. Aletras AH, Kellman P, Derbyshire JA, Arai AE: **ACUT2E TSE-SSFP: a hybrid method for T2-weighted imaging of edema in the heart.** *Magn Reson Med* 2008, **59**:229–35.

29. Friedrich MG, Strohm O, Schulz-Menger J, Marciniak H, Luft FC, Dietz R: **Contrast media-enhanced magnetic resonance imaging visualizes myocardial changes in the course of viral myocarditis.** *Circulation* 1998, **97**:1802–9.

30. Lauer B, Schannwell M, Kühl U, Strauer B-E, Schultheiss H-P: **Antimyosin autoantibodies are associated with deterioration of systolic and diastolic left ventricular function in patients with chronic myocarditis**. *J Am Coll Cardiol* 2000, **35**:11–18.

31. Cooper LT, Baughman KL, Feldman AM, Frustaci A, Jessup M, Kuhl U, Levine GN, Narula J, Starling RC, Towbin J, Virmani R: **The role of endomyocardial biopsy in the management of cardiovascular disease: a scientific statement from the American Heart Association, the American College of Cardiology, and the European Society of Cardiology. Endorsed by the Heart Failure Society of**. *J Am Coll Cardiol* 2007, **50**:1914–31.

32. Friedrich MG, Sechtem U, Schulz-Menger J, Holmvang G, Alakija P, Cooper LT, White J a, Abdel-Aty H, Gutberlet M, Prasad S, Aletras A, Laissy J-P, Paterson I, Filipchuk NG, Kumar A, Pauschinger M, Liu P: **Cardiovascular magnetic resonance in myocarditis: A JACC White Paper.** *J Am Coll Cardiol* 2009, **53**:1475–87.

33. Gutberlet M, Spors B, Thoma T, Bertram H, Denecke T, Felix R, Noutsias M, Schultheiss H-P, Kühl U: **Suspected chronic myocarditis at cardiac MR: diagnostic accuracy and association with immunohistologically detected inflammation and viral persistence.** *Radiology* 2008, **246**:401–9.

34. Ferreira VM, Piechnik SK, Dall'Armellina E, Karamitsos TD, Francis JM, Ntusi N, Holloway C, Choudhury RP, Kardos A, Robson MD, Friedrich MG, Neubauer S: **T(1) mapping for the diagnosis of acute myocarditis using CMR: comparison to T2-weighted and late gadolinium enhanced imaging.** *JACC Cardiovasc Imaging* 2013, **6**:1048–58.

35. Hinojar R, Foote L, Ucar E, Dabir D, Schnackenburg B, Higgins DM, Schaeffter T, Nagel E, Puntmann V: **Myocardial T2 mapping for improved detection of inflammatory myocardial involvement in acute and chronic myocarditis**. *J Cardiovasc Magn Reson* 2014, **16**(Suppl 1):O63.

36. McMurray JJ V, Adamopoulos S, Anker SD, Auricchio A, Böhm M, Dickstein K, Falk V, Filippatos G, Fonseca C, Gomez-Sanchez MA, Jaarsma T, Køber L, Lip GYH, Maggioni A Pietro, Parkhomenko A, Pieske BM, Popescu BA, Rønnevik PK, Rutten FH, Schwitter J, Seferovic P, Stepinska J, Trindade PT, Voors AA, Zannad F,

Zeiher A, Bax JJ, Baumgartner H, Ceconi C, Dean V, et al.: **ESC guidelines for the diagnosis and treatment of acute and chronic heart failure 2012: The Task Force for the Diagnosis and Treatment of Acute and Chronic Heart Failure 2012 of the European Society of Cardiology. Developed in collaboration with the Heart**. *Eur J Heart Fail* 2012, **14**:803–69.

37. Hsu K-H, Chi N-H, Yu H-Y, Wang C-H, Huang S-C, Wang S-S, Ko W-J, Chen Y-S: **Extracorporeal membranous oxygenation support for acute fulminant myocarditis: analysis of a single center's experience.** *Eur J Cardiothorac Surg* 2011, **40**:682–8.

38. Basso C, Carturan E, Corrado D, Thiene G: **Myocarditis and dilated cardiomyopathy in athletes: diagnosis, management, and recommendations for sport activity.** *Cardiol Clin* 2007, **25**:423–9, vi.

39. Pelliccia A, Fagard R, Bjørnstad HH, Anastassakis A, Arbustini E, Assanelli D, Biffi A, Borjesson M, Carrè F, Corrado D, Delise P, Dorwarth U, Hirth A, Heidbuchel H, Hoffmann E, Mellwig KP, Panhuyzen-Goedkoop N, Pisani A, Solberg EE, van-Buuren F, Vanhees L, Blomstrom-Lundqvist C, Deligiannis A, Dugmore D, Glikson M, Hoff PI, Hoffmann A, Hoffmann E, Horstkotte D, Nordrehaug JE, et al.: **Recommendations for competitive sports participation in athletes with cardiovascular disease: a consensus document from the Study Group of Sports Cardiology of the Working Group of Cardiac Rehabilitation and Exercise Physiology and the Working Group of My**. *Eur Heart J* 2005, **26**:1422–45.

40. Caforio ALP, Calabrese F, Angelini A, Tona F, Vinci A, Bottaro S, Ramondo A, Carturan E, Iliceto S, Thiene G, Daliento L: **A prospective study of biopsy-proven myocarditis: prognostic relevance of clinical and aetiopathogenetic features at diagnosis.** *Eur Heart J* 2007, **28**:1326–33.

41. Dennert R, Crijns HJ, Heymans S: **Acute viral myocarditis.** *Eur Heart J* 2008, **29**:2073–82.

42. Kindermann I, Kindermann M, Kandolf R, Klingel K, Bültmann B, Müller T, Lindinger A, Böhm M: **Predictors of outcome in patients with suspected myocarditis.** *Circulation* 2008, **118**:639–48.

43. Krueger GRF, Ablashi D V: **Human herpesvirus-6: a short review of its biological behavior.** *Intervirology* 2003, **46**:257–69.

44. Kühl U, Pauschinger M, Schwimmbeck PL, Seeberg B, Lober C, Noutsias M, Poller W, Schultheiss H-P: **Interferon-beta treatment eliminates cardiotropic viruses and improves left ventricular function in patients with myocardial persistence of viral genomes and left ventricular dysfunction.** *Circulation* 2003, **107**:2793–8.

45. Gullestad L, Aass H, Fjeld JG, Wikeby L, Andreassen AK, Ihlen H, Simonsen S, Kjekshus J, Nitter-Hauge S, Ueland T, Lien E, Froland SS, Aukrust P: **Immunomodulating Therapy With Intravenous Immunoglobulin in Patients With Chronic Heart Failure**. *Circulation* 2001, **103**:220–225.

46. Mason JW, O'Connell JB, Herskowitz A, Rose NR, McManus BM, Billingham ME, Moon TE: **A clinical trial of immunosuppressive therapy for myocarditis. The Myocarditis Treatment Trial Investigators.** *N Engl J Med* 1995, **333**:269–75.

47. Juenger J, Schellberg D, Kraemer S, Haunstetter A, Zugck C, Herzog W, Haass

M: **Health related quality of life in patients with congestive heart failure: comparison with other chronic diseases and relation to functional variables.** *Heart* 2002, **87**:235–41.

48. Braunwald E: **Heart failure.** *JACC Heart Fail* 2013, **1**:1–20.

49. Neubauer S: **The failing heart--an engine out of fuel.** *N Engl J Med* 2007, **356**:1140–51.

50. Bessman S, Geiger P: **Transport of energy in muscle: the phosphorylcreatine shuttle**. *Science (80-)* 1981, **211**:448–452.

51. Wallimann T, Tokarska-Schlattner M, Schlattner U: **The creatine kinase system and pleiotropic effects of creatine.** *Amino Acids* 2011, **40**:1271–96.

52. Guimbal C, Kilimann MW: **A Na(+)-dependent creatine transporter in rabbit brain, muscle, heart, and kidney. cDNA cloning and functional expression.** *J Biol Chem* 1993, **268**:8418–21.

53. Ingwall JS: **Energy metabolism in heart failure and remodelling.** *Cardiovasc Res* 2009, **81**:412–9.

54. Gupta A, Akki A, Wang Y, Leppo MK, Chacko VP, Foster DB, Caceres V, Shi S, Kirk JA, Su J, Lai S, Paolocci N, Steenbergen C, Gerstenblith G, Weiss RG: **Creatine kinase-mediated improvement of function in failing mouse hearts provides causal evidence the failing heart is energy starved.** *J Clin Invest* 2012, **122**:291–302.

55. Faller KME, Lygate C a, Neubauer S, Schneider JE: **(1)H-MR spectroscopy for analysis of cardiac lipid and creatine metabolism.** *Heart Fail Rev* 2013, **18**:657–68.

56. Ingwall JS, Weiss RG: **Is the failing heart energy starved? On using chemical energy to support cardiac function.** *Circ Res* 2004, **95**:135–45.

57. Osorio JC: **Impaired Myocardial Fatty Acid Oxidation and Reduced Protein Expression of Retinoid X Receptor-alpha in Pacing-Induced Heart Failure**. *Circulation* 2002, **106**:606–612.

58. Chandler MP, Kerner J, Huang H, Vazquez E, Reszko A, Martini WZ, Hoppel CL, Imai M, Rastogi S, Sabbah HN, Stanley WC: **Moderate severity heart failure does not involve a downregulation of myocardial fatty acid oxidation.** *Am J Physiol Heart Circ Physiol* 2004, **287**:H1538–43.

59. Nascimben L, Ingwall JS, Lorell BH, Pinz I, Schultz V, Tornheim K, Tian R: **Mechanisms for increased glycolysis in the hypertrophied rat heart.** *Hypertension* 2004, **44**:662–7.

60. Stanley WC, Recchia FA, Lopaschuk GD: **Myocardial substrate metabolism in the normal and failing heart.** *Physiol Rev* 2005, **85**:1093–129.

61. Ide T, Tsutsui H, Hayashidani S, Kang D, Suematsu N, Nakamura K, Utsumi H, Hamasaki N, Takeshita A: **Mitochondrial DNA damage and dysfunction associated with oxidative stress in failing hearts after myocardial infarction.** *Circ Res* 2001, **88**:529–35.

62. Marín-García J, Goldenthal MJ, Moe GW: **Abnormal cardiac and skeletal muscle mitochondrial function in pacing-induced cardiac failure.** *Cardiovasc Res* 2001, **52**:103–10.

63. Lewandowski ED: **Cardiac carbon 13 magnetic resonance spectroscopy: on the horizon or over the rainbow?** *J Nucl Cardiol* , **9**:419–28.

64. Starling RC, Hammer DF, Altschuld RA: **Human myocardial ATP content and in vivo contractile function.** *Mol Cell Biochem* 1998, **180**:171–7.

65. Shen W, Asai K, Uechi M, Mathier MA, Shannon RP, Vatner SF, Ingwall JS: **Progressive loss of myocardial ATP due to a loss of total purines during the development of heart failure in dogs: a compensatory role for the parallel loss of creatine.** *Circulation* 1999, **100**:2113–8.

66. Neubauer S, Horn M, Naumann A, Tian R, Hu K, Laser M, Friedrich J, Gaudron P, Schnackerz K, Ingwall JS: **Impairment of energy metabolism in intact residual myocardium of rat hearts with chronic myocardial infarction.** *J Clin Invest* 1995, **95**:1092–100.

67. Nascimben L, Ingwall JS, Pauletto P, Friedrich J, Gwathmey JK, Saks V, Pessina AC, Allen PD: **Creatine kinase system in failing and nonfailing human myocardium.** *Circulation* 1996, **94**:1894–901.

68. Schulze K: **Disturbance of myocardial energy metabolism in experimental virus myocarditis by antibodies against the adenine nucleotide translocator**. *Cardiovasc Res* 1999, **44**:91–100.

69. Bottomley PA, Weiss RG: **Non-invasive magnetic-resonance detection of creatine depletion in non-viable infarcted myocardium.** *Lancet* 1998, **351**:714–8.

70. den Hollander JA, Evanochko WT, Pohost GM: **Observation of cardiac lipids in humans by localized1H magnetic resonance spectroscopic imaging**. *Magn Reson Med* 1994, **32**:175–180.

71. Beckonert O, Keun HC, Ebbels TMD, Bundy J, Holmes E, Lindon JC, Nicholson JK: **Metabolic profiling, metabolomic and metabonomic procedures for NMR spectroscopy of urine, plasma, serum and tissue extracts.** *Nat Protoc* 2007, **2**:2692–703.

72. Tomlins AM, Foxall PJD, Lindon JC, Nicholson JK, Lynch MJ, Spraul M, Everett JR: **High resolution magic angle spinning 1H nuclear magnetic resonance analysis of intact prostatic hyperplastic and tumour tissues**. *Anal Commun* 1998, **35**:113–115.

73. Bollard M., Murray A., Clarke K, Nicholson J., Griffin J.: **A study of metabolic compartmentation in the rat heart and cardiac mitochondria using high-resolution magic angle spinning 1H NMR spectroscopy**. *FEBS Lett* 2003, **553**:73–78.

74. Schenetti L, Mucci A, Parenti F, Cagnoli R, Righi V, Tosi MR, Tugnoli V, Chimica D, Campi VG, Modena I-, Bologna S, Barbiano V: **HR-MAS NMR Spectroscopy in the Characterization of Human Tissues : Application to Healthy Gastric Mucosa**. :430–443.

75. ter Kuile BH, Westerhoff H V: **Transcriptome meets metabolome: hierarchical and metabolic regulation of the glycolytic pathway.** *FEBS Lett* 2001, **500**:169–71.

76. Martínez-Bisbal MC, Martí-Bonmatí L, Piquer J, Revert A, Ferrer P, Llácer JL, Piotto M, Assemat O, Celda B: **1H and 13C HR-MAS spectroscopy of intact biopsy samples ex vivo and in vivo 1H MRS study of human high grade**

gliomas. *NMR Biomed* 2004, **17**:191–205.

77. Wilson M, Davies NP, Grundy RG, Peet AC: **A quantitative comparison of metabolite signals as detected by in vivo MRS with ex vivo 1H HR-MAS for childhood brain tumours.** *NMR Biomed* 2009, **22**:213–9.

78. Millis K, Weybright P, Campbell N, Fletcher JA, Fletcher CD, Cory DG, Singer S: **Classification of human liposarcoma and lipoma using ex vivo proton NMR spectroscopy.** *Magn Reson Med* 1999, **41**:257–67.

79. Varma S, Bird R, Eskin M, Dolenko B, Raju J, Bezabeh T: **Detection of inflammatory bowel disease by proton magnetic resonance spectroscopy (1H MRS) using an animal model.** *J Inflamm (Lond)* 2007, **4**:24.

80. Sitter B, Lundgren S, Bathen TF, Halgunset J, Fjosne HE, Gribbestad IS: **Comparison of HR MAS MR spectroscopic profiles of breast cancer tissue with clinical parameters.** *NMR Biomed* 2006, **19**:30–40.

81. Chan ECY, Koh PK, Mal M, Cheah PY, Eu KW, Backshall A, Cavill R, Nicholson JK, Keun HC: **Metabolic profiling of human colorectal cancer using high-resolution magic angle spinning nuclear magnetic resonance (HR-MAS NMR) spectroscopy and gas chromatography mass spectrometry (GC/MS).** *J Proteome Res* 2009, **8**:352–61.

82. Tessem M-B, Swanson MG, Keshari KR, Albers MJ, Joun D, Tabatabai ZL, Simko JP, Shinohara K, Nelson SJ, Vigneron DB, Gribbestad IS, Kurhanewicz J: **Evaluation of lactate and alanine as metabolic biomarkers of prostate cancer using 1H HR-MAS spectroscopy of biopsy tissues.** *Magn Reson Med* 2008, **60**:510–6.

83. Lin A, Ross BD, Harris K, Wong W: **Efficacy of proton magnetic resonance spectroscopy in neurological diagnosis and neurotherapeutic decision making.** *NeuroRx* 2005, **2**:197–214.

84. Novak J, Wilson M, Macpherson L, Arvanitis TN, Davies NP, Peet AC: **Clinical protocols for ^{31}P MRS of the brain and their use in evaluating optic pathway gliomas in children.** *Eur J Radiol* 2014, **83**:e106–12.

85. Scheidegger O, Wingeier K, Stefan D, Graveron-Demilly D, van Ormondt D, Wiest R, Slotboom J: **Optimized quantitative magnetic resonance spectroscopy for clinical routine.** *Magn Reson Med* 2013, **70**:25–32.

86. Satoh H, Sperelakis N: **Review of some actions of taurine on ion channels of cardiac muscle cells and others.** *Gen Pharmacol* 1998, **30**:451–63.

87. Barba I, Jaimez-Auguets E, Rodriguez-Sinovas A, Garcia-Dorado D: **1H NMR-based metabolomic identification of at-risk areas after myocardial infarction in swine.** *MAGMA* 2007, **20**:265–71.

88. Marcinkiewicz J, Kontny E: **Taurine and inflammatory diseases. Amino Acids. 2014;46(1):7–20. doi:10.1007/s00726-012-1361-4.rine and inflammatory diseases.** *Amino Acids* 2014, **46**:7–20.

89. Kodama M, Matsumoto Y, Fujiwara M, Masani F, Izumi T, Shibata A: **A novel experimental model of giant cell myocarditis induced in rats by immunization with cardiac myosin fraction.** *Clin Immunol Immunopathol* 1990, **57**:250–62.

90. Yoshida Y, Shioi T, Izumi T: **Resveratrol ameliorates experimental autoimmune myocarditis.** *Circ J* 2007, **71**:397–404.

91. Veeraveedu PT, Watanabe K, Ma M, Palaniyandi SS, Yamaguchi K, Suzuki K, Kodama M, Aizawa Y: **Torasemide, a long-acting loop diuretic, reduces the progression of myocarditis to dilated cardiomyopathy.** *Eur J Pharmacol* 2008, **581**:121–31.

92. Smith SC: **Autoimmune myocarditis.** *Curr Protoc Immunol* 2001, **Chapter 15**:Unit 15.14.

93. Sato M, Toyozaki T, Odaka K, Uehara T, Arano Y, Hasegawa H, Yoshida K, Imanaka-Yoshida K, Yoshida T, Hiroe M, Tadokoro H, Irie T, Tanada S, Komuro I: **Detection of experimental autoimmune myocarditis in rats by 111In monoclonal antibody specific for tenascin-C.** *Circulation* 2002, **106**:1397–402.

94. Schmerler P, Jeuthe S, O H-Ici D, Wassilew K, Lauer D, Kaschina E, Kintscher U, Müller S, Muench F, Kuehne T, Berger F, Unger T, Steckelings UM, Paulis L, Messroghli D: **Mortality and morbidity in different immunization protocols for experimental autoimmune myocarditis in rats.** *Acta Physiol (Oxf)* 2014, **210**:889–98.

95. Gao H, Dong B, Jia J, Zhu H, Diao C, Yan Z, Huang Y, Li X: **Application of ex vivo (1)H NMR metabonomics to the characterization and possible detection of renal cell carcinoma metastases.** *J Cancer Res Clin Oncol* 2012, **138**:753–61.

96. Chen J, Wu Y V, Decarolis P, Connor RO, Somberg CJ, Singer S: **Resolution of Creatine and Phosphocreatine 1H Signals in Isolated Human Skeletal Muscle using HR-MAS 1H NMR**. 2009, **59**:1221–1224.

97. Bollard M., Murray a. ., Clarke K, Nicholson J., Griffin J.: **A study of metabolic compartmentation in the rat heart and cardiac mitochondria using high-resolution magic angle spinning 1H NMR spectroscopy**. *FEBS Lett* 2003, **553**:73–78.

98. Nakae I, Mitsunami K, Yoshino T, Omura T, Tsutamoto T, Matsumoto T, Morikawa S, Inubushi T, Horie M: **Clinical features of myocardial triglyceride in different types of cardiomyopathy assessed by proton magnetic resonance spectroscopy: comparison with myocardial creatine.** *J Card Fail* 2010, **16**:812–22.

99. Middleton D a, Bradley DP, Connor SC, Mullins PG, Reid DG: **The effect of sample freezing on proton magic-angle spinning NMR spectra of biological tissue.** *Magn Reson Med* 1998, **40**:166–9.

100. Mahrholdt H, Goedecke C, Wagner A, Meinhardt G, Athanasiadis A, Vogelsberg H, Fritz P, Klingel K, Kandolf R, Sechtem U: **Cardiovascular magnetic resonance assessment of human myocarditis: a comparison to histology and molecular pathology.** *Circulation* 2004, **109**:1250–8.

101. Nahrendorf M, Jaffer FA, Kelly KA, Sosnovik DE, Aikawa E, Libby P, Weissleder R: **Noninvasive vascular cell adhesion molecule-1 imaging identifies inflammatory activation of cells in atherosclerosis.** *Circulation* 2006, **114**:1504–11.

102. McAteer MA, Schneider JE, Ali ZA, Warrick N, Bursill CA, von zur Muhlen C, Greaves DR, Neubauer S, Channon KM, Choudhury RP: **Magnetic resonance imaging of endothelial adhesion molecules in mouse atherosclerosis using dual-targeted microparticles of iron oxide.** *Arterioscler Thromb Vasc Biol* 2008, **28**:77–83.

103. Neubauer S, Horn M, Cramer M, Harre K, Newell JB, Peters W, Pabst T, Ertl G, Hahn D, Ingwall JS, Kochsiek K: **Myocardial Phosphocreatine-to-ATP Ratio Is a Predictor of Mortality in Patients With Dilated Cardiomyopathy**. *Circulation* 1997, **96**:2190–2196.

104. Caus T, Kober F, Mouly-Bandini A, Riberi A, Métras DR, Cozzone PJ, Bernard M: **31P MRS of heart grafts provides metabolic markers of early dysfunction.** *Eur J Cardiothorac Surg* 2005, **28**:576–80.

105. Horn M, Frantz S, Remkes H, Laser a, Urban B, Mettenleiter a, Schnackerz K, Neubauer S: **Effects of chronic dietary creatine feeding on cardiac energy metabolism and on creatine content in heart, skeletal muscle, brain, liver and kidney.** *J Mol Cell Cardiol* 1998, **30**:277–84.

106. Ardenkjaer-Larsen JH, Fridlund B, Gram A, Hansson G, Hansson L, Lerche MH, Servin R, Thaning M, Golman K: **Increase in signal-to-noise ratio of > 10,000 times in liquid-state NMR.** *Proc Natl Acad Sci U S A* 2003, **100**:10158–63.

107. Kang S-M, Park J-C, Shin M-J, Lee H, Oh J, Ryu DH, Hwang G-S, Chung JH: **^{1}H nuclear magnetic resonance based metabolic urinary profiling of patients with ischemic heart failure.** *Clin Biochem* 2011, **44**:293–9.

108. Schaffer SW, Jong CJ, Ramila KC, Azuma J: **Physiological roles of taurine in heart and muscle.** *J Biomed Sci* 2010, **17 Suppl 1**(Suppl 1):S2.

109. Sharma S, Adrogue J V, Golfman L, Uray I, Lemm J, Youker K, Noon GP, Frazier OH, Taegtmeyer H: **Intramyocardial lipid accumulation in the failing human heart resembles the lipotoxic rat heart.** *FASEB J* 2004, **18**:1692–700.

110. Bilheimer DW, Buja LM, Parkey RW, Bonte FJ, Willerson JT: **Fatty acid accumulation and abnormal lipid deposition in peripheral and border zones of experimental myocardial infarcts.** *J Nucl Med* 1978, **19**:276–83.

111. Whitacre CC: **Sex differences in autoimmune disease.** *Nat Immunol* 2001, **2**:777–80.

112. Fairweather D, Frisancho-Kiss S, Rose NR: **Sex differences in autoimmune disease from a pathological perspective.** *Am J Pathol* 2008, **173**:600–9.

113. Pollard KM: **Gender differences in autoimmunity associated with exposure to environmental factors.** *J Autoimmun* 2012, **38**:J177–86.

114. Gangaplara A, Massilamany C, Steffen D, Reddy J: **Gender differences in the development of autoimmune myocarditis induced with cardiac myosin heavy chain-alpha, 334-352 in C57Bl/6 mice (BA15P.222)**. *J Immunol* 2014, **192**(1 Supplement):179.6.

115. Clayton JA, Collins FS: **Policy: NIH to balance sex in cell and animal studies.** *Nature* 2014, **509**:282–3.

116. Zucker I, Beery AK: **Males still dominate animal studies.** *Nature* 2010, **465**:690.

117. Wang C: **Radiology Characterization of Bone and Soft-Tissue Tumors with in Vivo 1 H MR Spectroscopy : Initial Results 1**. 2004:599–605.

118. Negendank WG, Sauter R, Brown TR, Evelhoch JL, Falini A, Gotsis ED, Heerschap A, Kamada K, Lee BC, Mengeot MM, Moser E, Padavic-Shaller KA, Sanders JA, Spraggins TA, Stillman AE, Terwey B, Vogl TJ, Wicklow K, Zimmerman RA: **Proton magnetic resonance spectroscopy in patients with glial tumors: a**

multicenter study. *J Neurosurg* 1996, **84**:449–58.

119. So WAH, Cox IJ: **Metabolic profiling of the rat liver after chronic ingestion magnetic of naphthylisothiocyanate spectroscopy using in vivo and ex vivo resonance**. 2012:1–34.

120. Woermann FG, McLean MA, Bartlett PA, Parker GJ, Barker GJ, Duncan JS: **Short echo time single-voxel 1H magnetic resonance spectroscopy in magnetic resonance imaging-negative temporal lobe epilepsy: different biochemical profile compared with hippocampal sclerosis.** *Ann Neurol* 1999, **45**:369–76.

121. Nelson SJ: **Multivoxel Magnetic Resonance Spectroscopy of Brain Tumors**. *Mol Cancer Ther* 2003, **2**:497–507.

122. Gross JD, Costa PR, Dubacq JP, Warschawski DE, Lirsac PN, Devaux PF, Griffin RG: **Multidimensional NMR in Lipid Systems. Coherence Transfer through J Couplings under MAS**. *J Magn Reson Ser B* 1995, **106**:187–190.

123. Lindon JC, Beckonert OP, Holmes E, Nicholson JK: **High-resolution magic angle spinning NMR spectroscopy: Application to biomedical studies**. *Prog Nucl Magn Reson Spectrosc* 2009, **55**:79–100.

124. Beckonert O, Coen M, Keun HC, Wang Y, Ebbels TMD, Holmes E, Lindon JC, Nicholson JK: **High-resolution magic-angle-spinning NMR spectroscopy for metabolic profiling of intact tissues.** *Nat Protoc* 2010, **5**:1019–32.

125. Albers MJ, Butler TN, Rahwa I, Bao N, Keshari KR, Swanson MG, Kurhanewicz J: **Evaluation of the ERETIC method as an improved quantitative reference for 1H HR-MAS spectroscopy of prostate tissue.** *Magn Reson Med* 2009, **61**:525–32.

Eidesstattliche Versicherung

„Ich, Frédéric Münch, versichere an Eides statt durch meine eigenhändige Unterschrift, dass ich die vorgelegte Dissertation mit dem Thema: „Metabolic profiling in experimental autoimmune myocarditis (EAM) in a rodent model using ex-vivo proton magic angle spinning magnetic resonance spectroscopy (1H-MAS-MRS) to detect myocardial injury“ selbstständig und ohne nicht offengelegte Hilfe Dritter verfasst und keine anderen als die angegebenen Quellen und Hilfsmittel genutzt habe.

Alle Stellen, die wörtlich oder dem Sinne nach auf Publikationen oder Vorträgen anderer Autoren beruhen, sind als solche in korrekter Zitierung (siehe „Uniform Requirements for Manuscripts (URM)“ des ICMJE -*www.**icmje**.org*) kenntlich gemacht. Die Abschnitte zu Methodik (insbesondere praktische Arbeiten, Laborbestimmungen, statistische Aufarbeitung) und Resultaten (insbesondere Abbildungen, Graphiken und Tabellen) entsprechen den URM (s.o) und werden von mir verantwortet.

Meine Anteile an etwaigen Publikationen zu dieser Dissertation entsprechen denen, die in der untenstehenden gemeinsamen Erklärung mit dem/der Betreuer/in, angegeben sind. Sämtliche Publikationen, die aus dieser Dissertation hervorgegangen sind und bei denen ich Autor bin, entsprechen den URM (s.o) und werden von mir verantwortet.

Die Bedeutung dieser eidesstattlichen Versicherung und die strafrechtlichen Folgen einer unwahren eidesstattlichen Versicherung (§156,161 des Strafgesetzbuches) sind mir bekannt und bewusst.“

Datum Unterschrift

Mein Lebenslauf wird aus datenschutzrechtlichen Gründen in der elektronischen Version meiner Arbeit nicht veröffentlicht.